

**EFFECTS OF
GLUTARALDEHYDE
CROSSLINKING AND
CHONDROITIN-6-SULFATE
UPON THE MECHANICAL
PROPERTIES AND IN VIVO
HEALING RESPONSE
OF AN ARTIFICIAL SKIN**

by

SUSAN DIANE FLYNN

SUBMITTED TO THE DEPARTMENT OF
CHEMICAL ENGINEERING IN PARTIAL
FULFILLMENT OF THE REQUIREMENTS FOR
THE DEGREE OF

BACHELOR OF SCIENCE

at the

MASSACHUSETTS INSTITUTE OF TECHNOLOGY

Copyright © 1983
May 1983

Signature of Author _____

Department of Chemical Engineering
May 27, 1983

Certified by _____

Dr Ioannis V. Yannas
Thesis Supervisor

Accepted by _____

Dr Charles M. Mohr
Chairman, Department Committee

MASSACHUSETTS INSTITUTE OF TECHNOLOGY

NOV 01 1984 ARCHIVES

EFFECTS OF GLUTARALDEHYDE CROSSLINKING
AND CHONDROITIN-6-SULFATE UPON
THE MECHANICAL PROPERTIES AND
IN VIVO HEALING RESPONSE
OF AN ARTIFICIAL SKIN

by

SUSAN DIANE FLYNN

Submitted to the Department of Chemical Engineering on
May 27, 1983 in partial fulfillment of the requirements
for the degree of Bachelor of Science.

Abstract

The effects of chondroitin-6-sulfate (GAG) and glutaraldehyde crosslinking upon the mechanical properties and the *in vivo* healing response of the Stage I artificial skin were examined. Two types of foams differing only in GAG content (0% and 8%) were manufactured with an identical extent of glutaraldehyde crosslinking. An additional foam containing 0% GAG was manufactured without glutaraldehyde crosslinking.

Utilizing an artificial skin graft placed in a full thickness skin wound in a guinea pig model, the crosslinked foams containing no GAG demonstrated a contraction rate of -5.6% wound area/day compared to a reduced contraction rate of -3.9% wound area/day demonstrated by the crosslinked foams containing GAG. An increased contraction rate of -5.9% wound area/day was exhibited by the uncrosslinked foams containing no GAG.

50% closure of the original wound was seen on Day 19 with the crosslinked foams containing GAG. A three day advance in 50% wound closure on Day 16 was demonstrated by the crosslinked foams containing no GAG compared to the material containing GAG. The uncrosslinked foams which contained no GAG were seen to have 50% wound closure on Day 12.

The onset of contraction for both types of crosslinked foams occurred on Day

14. The uncrosslinked foams containing no GAG were seen to begin wound contraction as early as Day 5, indicating a nine day increase in the onset of wound contraction.

Thesis Supervisor: Dr Ioannis V. Yannas
Title: Professor of Polymer Science & Engineering

Acknowledgements

I would like to thank Dr. I.V. Yannas for the great amount of insight and understanding he has lent to this research. His assistance was greatly appreciated.

I would also like to acknowledge two people without whom this research would not have been possible: Mr. Eugene Skrabut and Dr. Dennis Orgill. Their advice and assistance on matters both small and large provided the support for the completion of this work.

Thanks go to Jude Colt, John Emy, and James Kirk for their invaluable assistance at all hours with the animal studies and to Robert Wilson for performing the $1/\tau$ testing used in this work.

Finally, I would like to thank Joseph Izatt for both helping me to type this thesis and giving me the support to finish it.

This research was partially supported by a Sigma Xi grant received from the Undergraduate Research Opportunities Program at the Massachusetts Institute of Technology.

Table of Contents

| | |
|---|-----------|
| Abstract | 2 |
| Acknowledgements | 4 |
| Table of Contents | 5 |
| List of Figures | 7 |
| List of Tables | 9 |
| 1. Introduction | 10 |
| 2. Materials and Methods | 18 |
| 2.1 Materials | 18 |
| 2.2 Methods | 19 |
| 2.2.1 Preparation of Control Stage I Membrane | 19 |
| 2.2.2 Preparation of a No GAG Stage I Membrane | 24 |
| 2.2.3 Preparation of a NO GAG, Uncrosslinked Stage I Membrane | 26 |
| 2.2.4 Dry Weights: Percent Solids | 28 |
| 2.2.5 Infrared Spectroscopy: Collagen Helicity | 29 |
| 2.2.6 Transmission Electron Microscopy: Collagen Banding | 30 |
| 2.2.7 Scanning Electron Microscopy: Porosity | 31 |
| 2.2.8 M _c Testing: Crosslink Density | 33 |
| 2.2.9 1/ τ Testing: Collagenase Degradation | 35 |
| 2.2.10 Hexosamine Assay: Percent GAG | 36 |
| 2.2.11 <i>In Vivo</i> Response | 37 |
| 3. Results | 41 |
| 3.1 Percent Solids | 41 |
| 3.2 Collagen Helicity | 42 |
| 3.3 Collagen Banding | 42 |
| 3.4 Porosity | 45 |
| 3.5 Crosslink Density | 45 |
| 3.6 Collagenase Degradation | 49 |
| 3.7 Percent GAG | 50 |
| 3.8 Histology: Cellular Infiltration | 51 |
| 3.9 Contraction/Epithelialization | 64 |
| 4. Discussion | 73 |
| 4.1 Effects of Glutaraldehyde Crosslinking and Chondroitin-6-Sulfate Upon the Mechanical Properties and <i>In Vivo</i> Response of an Artificial Skin | 73 |

5. Conclusions

81

References

83

List of Figures

| | | |
|---------------------|--|----|
| Figure 1-1: | Schematic of Stage I Artificial Skin ⁹ | 12 |
| Figure 1-2: | Reduction in Area of Full Thickness Skin Wounds In Guinea Pigs. Comparison of wounds treated with Stage I Artificial Skin to untreated wounds ⁹ | 14 |
| Figure 1-3: | Composite of Reduction in Wound Area of Full Thickness Skin Wounds in Guinea Pigs. Comparison of crosslinked and uncrosslinked skin grafts. ¹⁰ | 15 |
| Figure 2-1: | Testing Procedures During Skin Processing | 20 |
| Figure 2-2: | Protocol for Control Stage I Membrane (GAG, Crosslinked) | 21 |
| Figure 2-3: | Protocol for No GAG Stage I Membrane (No GAG, Crosslinked) | 25 |
| Figure 2-4: | Protocol for No GAG, Uncrosslinked Stage I Membrane | 27 |
| Figure 2-5: | Collagen Banding Levels | 32 |
| Figure 2-6: | Determination of the Porosity of a Collagen Matrix. Diagram of pore outline of photomicrograph. | 34 |
| Figure 2-7: | Measurement of Wound Contraction Exhibited by Grafted Woundbed. Comparison of wound area at Day 0 to contracted wound. | 40 |
| Figure 3-1: | TEM Photomicrograph of Collagen-GAG Slurry at pH 3 | 43 |
| Figure 3-2: | TEM Photomicrograph of Collagen-No GAG Slurry at pH 3 | 44 |
| Figure 3-3: | SEM Photomicrographs of Control GAG, Crosslinked Membranes | 46 |
| Figure 3-4: | SEM Photomicrographs of No GAG, Crosslinked Membranes | 47 |
| Figure 3-5: | SEM Photomicrographs of No GAG, Uncrosslinked Membranes | 48 |
| Figure 3-6: | Histological Sections: Control GAG, Crosslinked Membranes - Day 14 D=Dermis, E=Epidermis, G=Graft, P=Panniculus Adiposus | 57 |
| Figure 3-7: | Histological Sections: Control GAG, Crosslinked Membranes - Day 28 D=Dermis, E=Epidermis, G=Graft, P=Panniculus Adiposus | 58 |
| Figure 3-8: | Histological Sections: No GAG, Crosslinked Membranes - Day 14 D=Dermis, E=Epidermis, G=Graft, P=Panniculus Adiposus | 60 |
| Figure 3-9: | Histological Sections: No GAG, Crosslinked Membranes - Day 28 D=Dermis, E=Epidermis, G=Graft, P=Panniculus Adiposus | 61 |
| Figure 3-10: | Histological Sections: No GAG, Uncrosslinked Membranes - Day 14 D=Dermis, E=Epidermis, G=Graft, P=Panniculus Adiposus | 62 |

| | |
|---|----|
| Figure 3-11: Histological Sections: No GAG, Uncrosslinked Membranes - Day 28 D=Dermis, E=Epidermis, G=Graft, P=Panniculus Adiposus | 63 |
| Figure 3-12: Composite of Wound Reduction Curves: Comparison of GAG, Crosslinked Membrane, No GAG, Crosslinked Membrane, and Untreated Wound | 65 |
| Figure 3-13: Composite of Wound Reduction Curves: Comparison of GAG, Crosslinked Membrane, No GAG, Uncrosslinked Membrane, and Untreated Wound | 66 |
| Figure 3-14: Wound Contraction of Control GAG, Crosslinked Membranes: Days 14, 18, 24, and 33 | 67 |
| Figure 3-15: Wound Contraction of No GAG, Crosslinked Membranes: Days 14, 18, 24, and 33 | 68 |
| Figure 3-16: Wound Contraction of No GAG, Uncrosslinked Membranes: Days 7, 14, 18, and 28 | 69 |
| Figure 3-17: Composite Wound Contraction Curve | 71 |

List of Tables

| | | |
|----------------------|---|----|
| Table 3-I: | Percent Solids | 41 |
| Table 3-II: | Collagen Helicity | 42 |
| Table 3-III: | Length Average Banding | 42 |
| Table 3-IV: | Porosity | 45 |
| Table 3-V: | Crosslink Density | 49 |
| Table 3-VI: | Collagenase Degradation | 50 |
| Table 3-VII: | Glycosaminoglycan Content | 51 |
| Table 3-VIII: | Animal Study Data | 52 |
| Table 3-IX: | Histological Findings - GAG, Crosslinked Membranes | 54 |
| Table 3-X: | Histological Findings - No GAG, Crosslinked Membranes | 55 |
| Table 3-XI: | Histological Findings - No GAG, Uncrosslinked Membranes | 56 |
| Table 3-XII: | Linear Regression of Contraction Data | 72 |
| Table 4-I: | Contraction Data | 77 |

Chapter 1

Introduction

An estimated 130,000 individuals are hospitalized annually for injuries resulting from exposure to fire¹. Of these, 70% suffer extensive skin damage. The immediate trauma of the burn patient is often fatal unless managed quickly and effectively. Those burn victims who survive the threats of extreme fluid loss and bacterial infection permanently bear scars and contractures that are crippling both physically and emotionally.

There are presently many avenues of treatment with varying degrees of effectiveness available for the burn victim. Autografting has been the preferred method of burn treatment due to the lack of contractures resultant from its usage. Autografting requires the availability of the patient's own healthy skin for grafting in the damaged area. If the patient bears burns over more than 50% of his body, the treatment is limited by the availability of the skin and alternate means of wound management must be utilized².

Both allografts and xenografts are used in the short term management of severe burns when adequate autograft is not available. Due to their rejection by the patient's immune system, the allograft and xenograft are only used as temporary wound coverings².

There exists a need for a temporary physiologic replacement for skin which will serve the function of a patient's natural skin without eliciting an immune response. The design parameters involved include regulating fluid loss, preventing bacterial proliferation, and being biologically inert³. Past materials

composed of synthetic polymers and reconstituted collagen have been examined without success⁴⁻⁶.

Recently, the development of a collagen-glycosaminoglycan membrane reinforced with an upper layer of silicone sheeting has fulfilled the need for a temporary physiologic skin replacement. The Stage I artificial skin, as seen in Figure 1-1, is able to meet both the immediate and short term needs of the burn victim due to its material properties^{3,7}. The fluid loss of the wound is regulated by the upper layer of the silicone sheeting. The silicone sheeting also provides a support into which the surgeon is able to suture without damaging the underlying collagen-glycosaminoglycan layer. The bottom collagen-glycosaminoglycan matrix is weakly antigenic. Its wetting ability prevents the formation of air pockets underneath the membrane while allowing adhesion to the wound surface. As time progresses, the Stage I artificial skin permits the formation of a neodermis following infiltration of mesenchymal cells into the bottom of the matrix and synthesis of new tissue. While the neodermis is forming, the collagen-glycosaminoglycan complex is being degraded by tissue collagenases. This creates a steady-state situation in which the artificial membrane is replaced by the patient's neodermal connective tissue. Upon closure of the neodermis and removal of the silicone layer, the surgeon is able to meshgraft a thin autoepidermal layer over the neodermis for complete closure of the wound.

A long term effect of a severe skin injury that must be considered in the design of an artificial skin is contraction. Contraction is the reduction of wound area due to healing of a full thickness injury by gradual approximation of the wound edges⁸. Contraction of a full thickness wound is often responsible for extreme contractures which cause both scarring and loss of

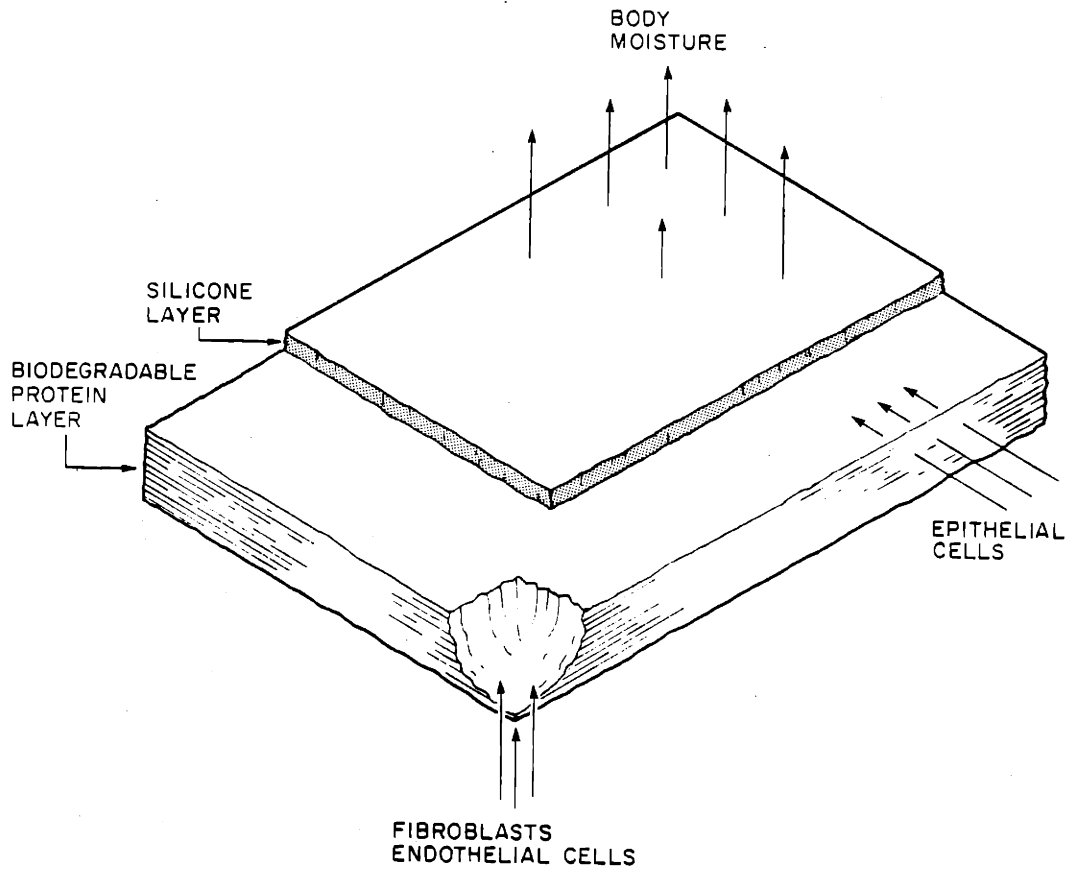


Figure 1-1: Schematic of Stage I Artificial Skin⁹

mobility. These long term results of severe burns scar the victim physically and emotionally for life. A material which could delay or prevent the onset of contraction would be significant in the treatment of a burn victim.

The Stage I artificial skin has also been found to significantly delay the onset of wound contraction in a guinea pig model⁹. As seen in Figure 1-2, a delay of fifteen days in contraction is demonstrated through the comparison of the closure of a full thickness wound treated with Stage I artificial skin to the closure of a similar wound left untreated. However, the actual mechanism behind the delay in the contraction kinetics has yet to be clearly elucidated.

Chen¹⁰ demonstrated that the glutaraldehyde crosslinking of the Stage I artificial skin is responsible for a four day delay in the onset of wound contraction. The result, obtained from the comparison of the contraction kinetics of a crosslinked membrane and a non-crosslinked membrane, is diagrammed in Figure 1-3. Glutaraldehyde crosslinking creates a greater crosslink density in the membrane. This result suggests that other factors, in combination with increased crosslink density, are responsible for the fifteen day delay in the onset of wound contraction.

Other factors have been hypothesized to affect wound contraction kinetics. The *in vivo* response to the presence of chondroitin-6-sulfate was chosen for examination. Chondroitin-6-sulfate is a glycosaminoglycan (GAG) containing disaccharide repeat units consisting of D-glucuronic acid and the O-sulfate derivative of N-acetyl D-galactosamine. Studies have indicated that glycosaminoglycans are capable of binding to collagen at physiological conditions via an electrostatic interaction. Each collagen monomer is capable of binding two to five polysaccharide chains, depending on the type of glycosaminoglycan¹¹.

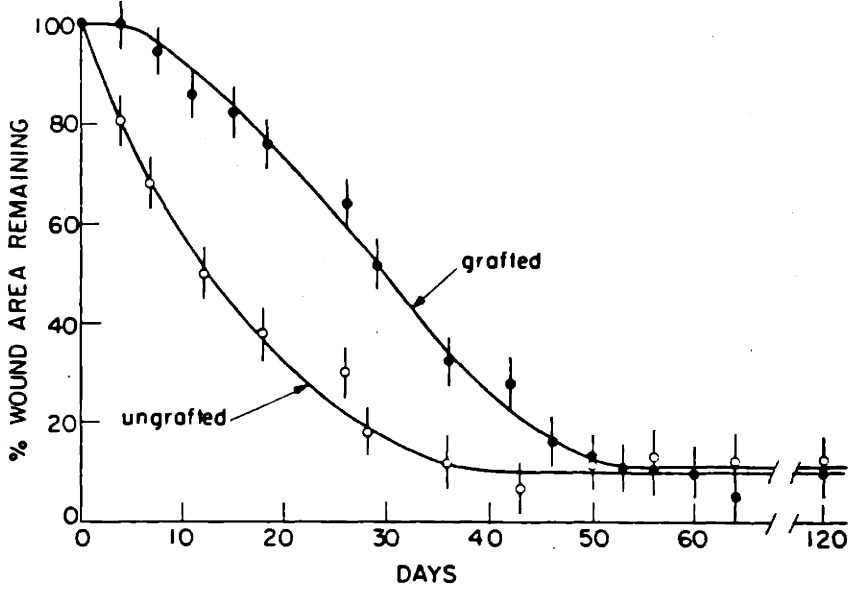


Figure 1-2: Reduction in Area of Full Thickness Skin Wounds In Guinea Pigs. Comparison of wounds treated with Stage I Artificial Skin to untreated wounds⁹

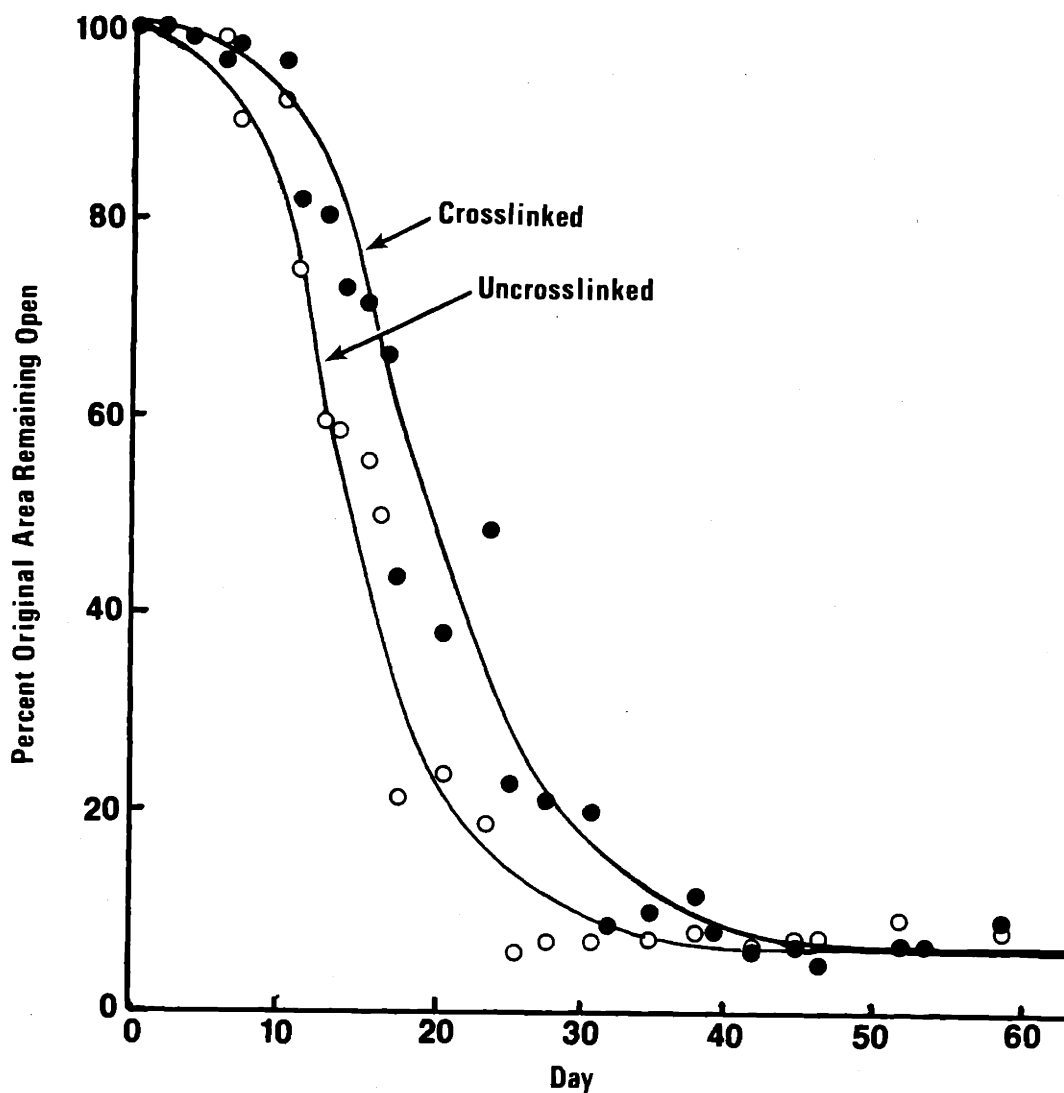


Figure 1-3: Composite of Reduction in Wound Area of Full Thickness Skin Wounds in Guinea Pigs. Comparison of crosslinked and uncrosslinked skin grafts.¹⁰

Work by Huang¹² has demonstrated that the presence of covalently bound GAG in a collagen membrane induces a reduction in the *in vitro* enzymatic degradation rate of the membrane by collagenase. The reduction of the collagenase degradation rate in an artificial membrane permits the maintenance of a longer lasting scaffolding for cellular infiltration.

The addition of chondroitin-6-sulfate to the collagen slurry of the Stage I artificial skin induces precipitation of the collagen and formation of a collagen-GAG complex⁹. Chondroitin-6-sulfate has been found to remain in the collagen matrix upon processing. The effect of the collagen-GAG interaction upon the mechanical strength and *in vivo* response of the Stage I artificial skin was examined to determine if its behavior followed Huang's findings.

To study the effect of chondroitin-6-sulfate, a GAG-free membrane was prepared following the standard protocol, without the addition of chondroitin-6-sulfate⁹. Through minor processing variations, the resultant membrane exhibited mechanical properties similar to those of the Stage I GAG membrane; including porosity, banding, and crosslink density. The no-GAG foam differed significantly only by an increased *in vitro* collagenase degradation rate¹³. Grafting of the material on guinea pigs followed to determine the contraction kinetics and cellular infiltration. A comparison of the contraction kinetics exhibited by wounds treated with GAG and no-GAG materials would indicate if the presence of GAG delayed the onset of contraction. Further, the histological findings from the two studies would reveal the influence of GAG upon the matrix scaffolding and the resultant cellular infiltration.

A final question was whether the effects of glutaraldehyde crosslinking and glycosaminoglycan content upon the *in vivo* response of the artificial

membrane were independent phenomena. To examine this, a no-GAG foam was prepared and processed without glutaraldehyde crosslinking. Efforts were made to keep all material properties except crosslink density and collagenase degradation consistent with the Stage I artificial skin. The material was grafted on guinea pigs and the *in vivo* response followed. The resultant contraction data would indicate if the delay in the onset of wound healing was a sum of the delays induced by the presence of chondroitin-6-sulfate and glutaraldehyde crosslinking individually. Histological data would allow the correlation of cellular infiltration to the wound contraction exhibited at the time of sacrifice.

The studies proposed attempt to elucidate a clear mechanism for the fifteen day delay in the onset of wound contraction. By examining select processing variables, their effects on the mechanism of contraction delay may be studied.

Chapter 2

Materials and Methods

2.1 Materials

Bovine hide collagen, obtained from the U.S. Department of Agriculture, was used throughout the experimentation. Before receipt, the collagen was processed as outlined by Komanowsky, et al¹⁴. The collagen was refrigerated at 4°C to prevent possible denaturation.

A deionizing organic adsorption system (Hydro Services and Supplies, Inc., Durham, N.C.) was used to provide deionized water for all phases of the experimentation.

Acetic acid (0.05 M, pH 3) was used for the dispersion and rehydration steps of the membrane production. Solutions were prepared by the dilution of glacial acetic acid (analytical reagent, Mallinckrodt, Inc., Paris, KY) with deionized water.

A 0.1% w/v solution of chondroitin-6-sulfate (type C, sodium salt from shark cartilage, Sigma Chemical Company, St. Louis, MO) prepared with acetic acid was used in the studies. The glycosaminoglycan was refrigerated at 4°C to prevent bacterial proliferation.

Siliconization of the membrane was accomplished by adhering silicone sheeting (medical grade, 7 mil Silastic reinforced sheeting, Dow Corning, Midland, MI) to the collagen-GAG membrane with 355 Medical adhesive (Dow Corning, Midland, MI).

A 0.25% solution of glutaraldehyde (practical grade, Eastman Kodak Company, Rochester, N.Y.) in 0.05 M acetic acid was the crosslinking agent used.

The processed membranes were packaged in 70% isopropanol (MCB Manufacturing Chemists, Inc., Cincinnati, OH) prepared with deionized water.

Phosphate buffered saline (PBS) was prepared for storage of the animal grafts prior to surgery. 50 ml of 10X concentrated PBS (Dulbecco's Phosphate Buffered Saline, without calcium and magnesium, M.A. Bioproducts, Walkersville, MD) was diluted with 450 ml of sterile deionized water (M.A. Bioproducts, Walkersville, MD).

2.2 Methods

The processing of the collagen membranes used in the experimental studies closely followed the Stage I artificial skin protocol outlined by Yannas⁹. As illustrated in Figure 2-1, testing was performed at various stages in the processing to determine the material properties of the collagen membranes. The testing determined if membranes were produced that differed significantly in only one material property from the control Stage I material. This permitted a direct observation of the effect of the varied material property on the *in vivo* response.

2.2.1 Preparation of Control Stage I Membrane

Bovine hide collagen was shredded and ground to a 20 Mesh particle size utilizing a Wiley Mill (Arthur H. Thomas, Co., Philadelphia, PA). Liquid

Figure 2-1: Testing Procedures During Skin Processing

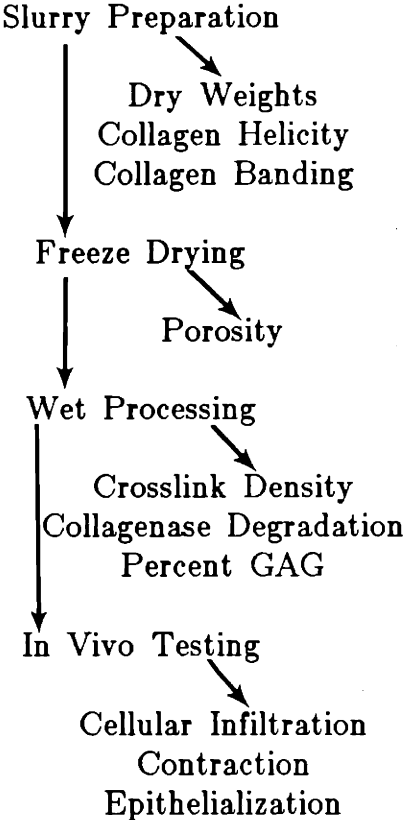
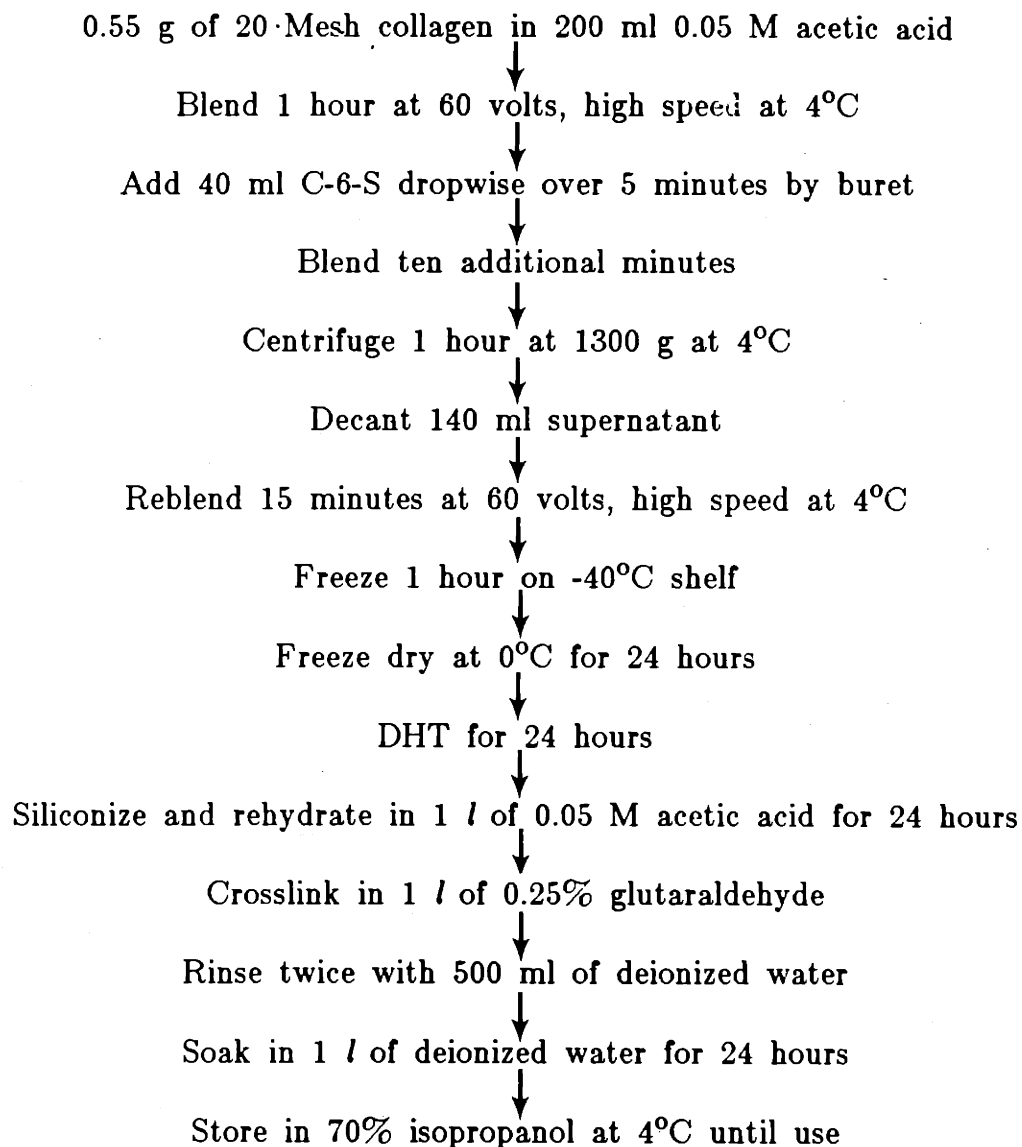


Figure 2-2: Protocol for Control Stage I Membrane (GAG, Crosslinked)

nitrogen was passed through the mill immediately preceding and during grinding to prevent denaturation of the collagen.

200 ml of acetic acid (0.05 M, pH 3) was placed in a cooled blender (Model 8590, Eberbach Corporation, Ann Arbor, MI) jacketed with a glycol/water mixture at 4°C. A circulating cooler (model RC-2T, Brinkmann, Westbury, CT) was used to maintain the temperature during the experimentation. 0.55 g of 20 Mesh collagen was added to the acetic acid and the dispersion blended for one hour at a high speed setting with 60 volts.

Upon completion, 40 ml of chondroitin-6-sulfate (0.1% solution in 0.05 M acetic acid, pH 3) were dripped into the blending dispersion over a five minute period. A co-precipitation of the collagen-glycosaminoglycan complex followed. Ten minutes additional blending were allowed for complete mixing.

The 240 ml dispersion was decanted and placed in a refrigerated centrifuge (model CRU-5000, Damon, International Equipment Co., Needham Heights, MA). The slurries were spun at 1300 g for one hour at 4°C. 140 ml of the resultant supernatant was withdrawn, leaving a concentrated 100 ml slurry.

Immediately preceding freeze drying, the slurry was reblended for fifteen minutes at high speed, 60 volts in a cooled Eberbach blender.

The slurries were freeze dried to produce a collagen foam. An aluminum tray was filled with 2 ml of slurry per square inch of pan surface area. The tray was placed in the freeze drier (model 10 MRPC freeze drier mounted on Freeze Mobile 12, The Virtis Company, Inc., Gardiner, N.Y.) on a -40°C shelf to freeze for one hour. The freeze drying chamber was then evacuated. When the vacuum reached 200 millitorr, the shelf temperature was set to 0°C

and the material allowed to freeze dry for twenty four hours.

Removal of the collagen foam from the freeze drier followed its equilibration to room temperature under vacuum. The foam was packaged in aluminum foil and dehydrothermally treated for twenty four hours under vacuum in a 105°C oven (Model 201, Fisher IsoTemp Vacuum Oven, Pittsburgh, PA). The procedure both sterilized the foam and dehydrothermally crosslinked the collagen matrix. Following treatment, the foam was desiccated until further use.

Processing was continued under sterile conditions in a laminar air flow hood (Tenney Eng. Inc., Union, N.J.). The foam was siliconized by spreading 355 Medical adhesive on both the smooth side of the Silastic sheeting and the collapsed side (air side) of the foam with a gauze. Gentle pressure was used to adhere the two together. A minimum of five minutes was allowed for drying before the continuation of the processing.

The membrane was rehydrated by immersion in acetic acid (0.05 M, pH 3). The foam was first placed pore side (pan side) down in one liter of acetic acid for fifteen seconds before placing silicone side down for twenty four hours. During the interim, excess air was removed from the foam by gentle pressure with a sterile gloved hand.

The foam was next placed silicone side down in one liter of 0.25% glutaraldehyde (pH 3) for twenty four hours. The glutaraldehyde both induced crosslinking in the collagen matrix and further enhanced the sterility of the material.

To remove the unbound glutaraldehyde, the foam was rinsed twice in 500 ml of deionized water before soaking for twenty four hours in one liter of

deionized water.

Upon completion of processing, the artificial membrane was packaged in 70% isopropanol and refrigerated at 4°C until use.

2.2.2 Preparation of a No GAG Stage I Membrane

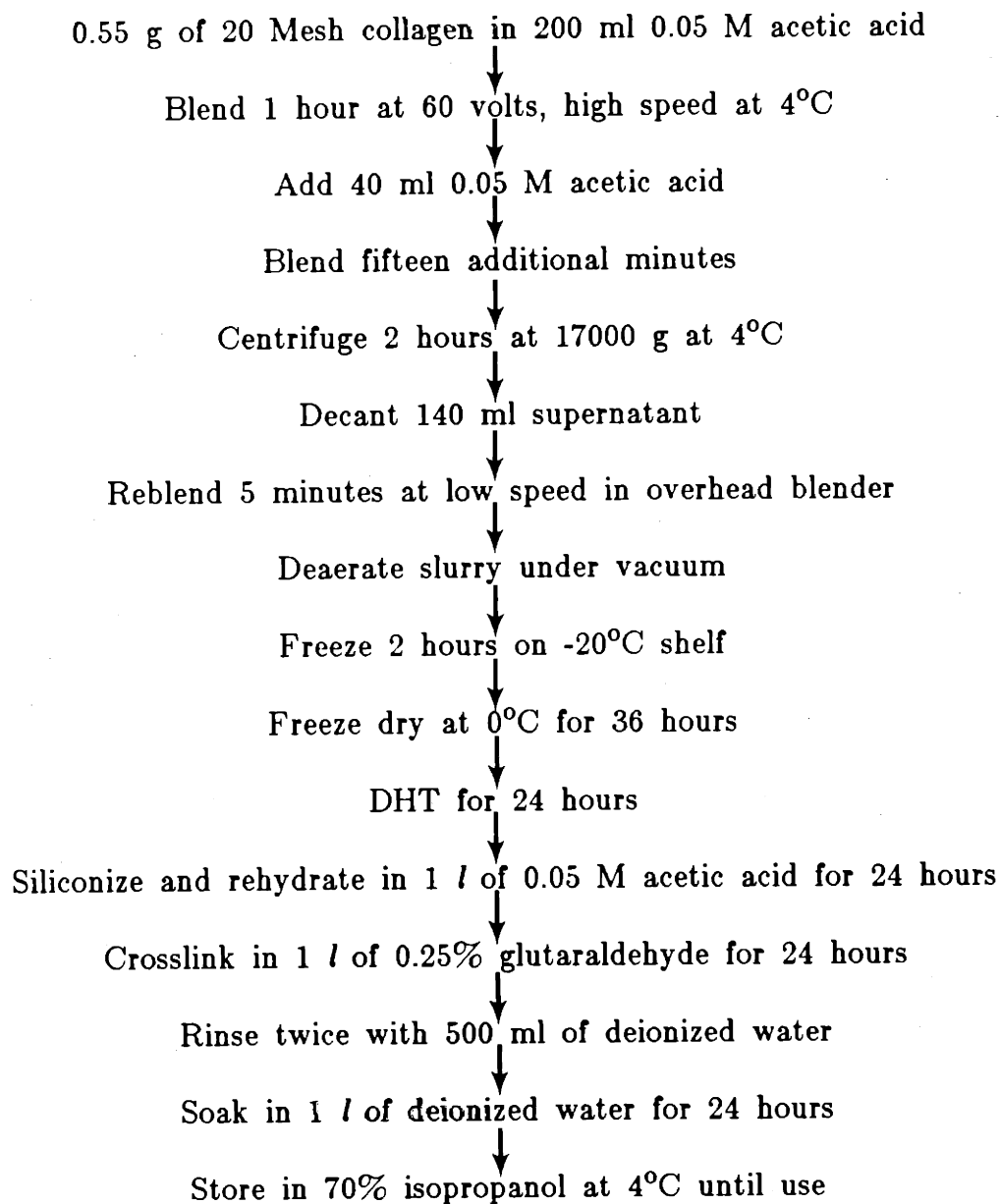
Bovine hide collagen was ground to a 20 mesh particle size. 200 ml of acetic acid (0.05 M, pH 3) was placed in a blender jacketed with 4°C coolant. 0.55 g of 20 mesh collagen were added to the acetic acid and the dispersion blended one hour at a 60 volt, high speed setting.

In place of the chondroitin-6-sulfate, 40 ml of acetic acid were placed in the blending dispersion. The dispersion was allowed to blend an additional fifteen minutes, both for complete mixing and consistency with the standard protocol.

The 240 ml dispersion was decanted. As the lack of glycosaminoglycan caused an increased viscosity and the lack of collagen precipitation, the slurry was centrifuged at 17,000 g for two hours at 4°C in an high speed centrifuge (Model J-21B with a JA 10 rotor, Beckman Instruments, Inc., Palo Alto, CA). A concentrated slurry was prepared by decanting 140 ml of supernatant.

The slurry was reblended for five minutes prior to freeze drying in an overhead blender at low speed, 45 volts. Excess air bubbles in the slurry created by reblending were removed by vacuum deaeration.

An aluminum tray was filled with 2 ml of slurry per square inch of pan surface area. The slurry was frozen on a -20°C shelf in the freeze drier for two hours before evacuation of the chamber. Upon attaining a vacuum of 200 millitorr, the shelf temperature was set to 0°C and the material allowed to

Figure 2-3: Protocol for No GAG Stage I Membrane (No GAG, Crosslinked)

freeze dry for thirty six hours.

The remaining processing followed that outlined for the control Stage I membrane. Briefly, the foam was dehydrothermally treated and dessicated until use. Wet processing consisted of siliconization with Silastic sheeting, rehydration in acetic acid (0.05 M, pH 3) for twenty four hours, crosslinking in .25% glutaraldehyde (pH 3) for twenty four hours, rinsing in deionized water for twenty four hours, and packaging in 70% isopropanol.

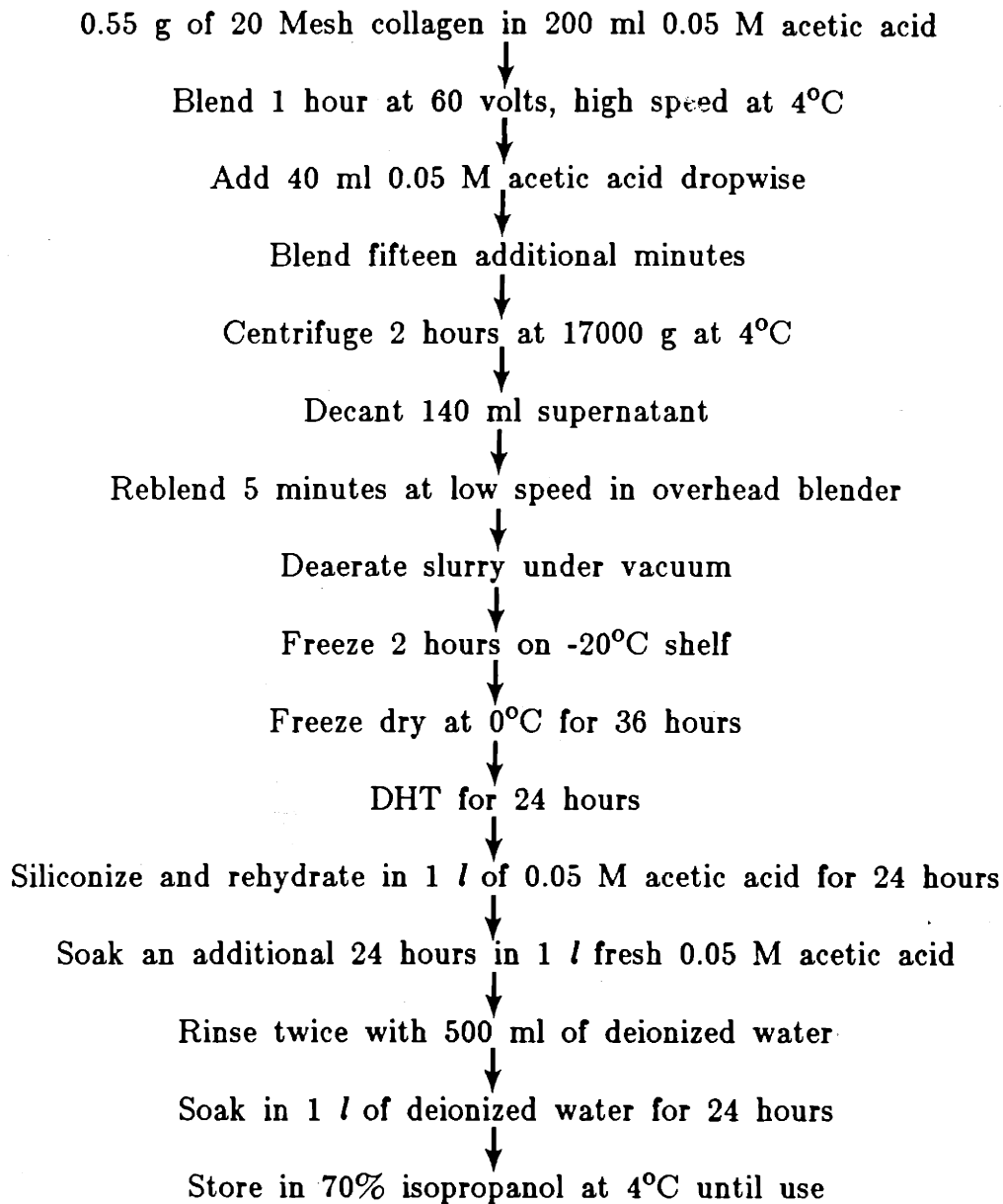
2.2.3 Preparation of a NO GAG, Uncrosslinked Stage I Membrane

The foam was prepared up to the wet processing stages as outlined for the no-GAG Stage I membrane. 0.55 g of 20 mesh collagen was dispersed in 200 ml of acetic acid (0.05 M, pH 3), with the addition of 40 ml of acetic acid following one hour of blending. The dispersion was centrifuged at 17,000 g for two hours at 4°C. 140 ml of supernatant was decanted. After reblending and freezing the slurry on a -20°C shelf, the material was freeze dried thirty six hours. The material was dehydrothermally treated and dessicated until use.

Utilizing sterile technique, the foam was siliconized with Silastic sheeting by adhesion to the collapsed side of the foam with 355 Medical adhesive. Five minutes were allowed for drying before the continuation of processing.

The membrane was rehydrated by immersion in one liter of acetic acid (0.05 M, pH 3). The porous side of the foam was first placed down in the solution followed by twenty four hour immersion silicone side down.

In place of crosslinking with glutaraldehyde, the membrane was immersed silicone side down in one liter of fresh acetic acid (0.05 M, pH 3) for an additional twenty four hours.

Figure 2-4: Protocol for No GAG, Uncrosslinked Stage I Membrane

The membrane was rinsed twice with 500 ml of deionized water before twenty four hours of soaking in one liter of deionized water.

The membrane was packaged in 70% isopropanol and stored at 4°C until further use.

2.2.4 Dry Weights: Percent Solids

The percent solids represents the percentage of collagen and glycosaminoglycan present in the concentrated collagen slurry before freeze drying. To determine this value, slurry was pipetted into a previously weighed aluminum weigh boat. The combined weight of the slurry and boat was next taken before placing the sample in a drying oven (Model 201, Fisher IsoTemp Vacuum Oven, Pittsburgh, PA) for twenty four hours at 105 °C. This step removed all the moisture from the slurry. Upon completion of drying, the dry slurry and boat were weighed. The percent solids was calculated by dividing the dry weight of the slurry by its total weight before moisture removal as seen below.

$$\text{Percent Solids} = 100((W_3 - W_1)/(W_2 - W_1))$$

where:

$$\begin{aligned} W_1 &= \text{Weight of weighing pan empty (g)} \\ W_2 &= \text{Weight of pan and slurry before drying (g)} \\ W_3 &= \text{Weight of pan and slurry after drying (g)} \end{aligned}$$

All samples were weighed on an analytical balance (Type H6, Mettler Instrument Corp., Hightstown, New Jersey).

2.2.5 Infrared Spectroscopy: Collagen Helicity

Examination of the infrared bands of a collagen foam at the frequency levels of 1450 cm^{-1} and 1235 cm^{-1} yields significant information on the helical nature of the collagen specimen. The 1235 cm^{-1} band varies with respect to the native content of the specimen. As the variation of the 1450 cm^{-1} band is dependent on the protein content regardless of helicity, it serves as an internal standard. Utilizing the relationship existing between the two band ranges, a mathematical approximation has been derived equating the relative value obtained to a percentage of helicity¹⁶.

The procedure for the determination of collagen helicity was originally developed by Sung¹⁶. The following modification of the procedure was used in the present work due to material constraints.

An aliquot of concentrated collagen slurry was agitated vigorously for five minutes. A 3 ml or 5 ml sample of slurry was placed in a plastic boat and diluted up to 12 ml by addition of acetic acid (0.05 M, pH 3). The suspensions were allowed to air dry in a laminar air flow hood for a minimum of twenty four hours to permit evaporation of the acetic acid. Upon drying, the films were carefully removed from the boats and mounted in cardboard holders. Prior to use, the films were dessicated to prevent excess water adsorption.

The films were run on an infrared spectrophotometer (Perkin-Elmer 283B, Perkin-Elmer Corporation, Norwalk, CT) under normal conditions with a twelve minute scan time. Upon completion of the infrared spectrum, the absorbances of the bands falling at 1450 cm^{-1} and 1235 cm^{-1} were calculated following the methods described by Sung¹⁶. Briefly, the baseline of 1450 cm^{-1}

band was drawn by connecting the maximum peaks found at approximately 1485 cm^{-1} and 1360 cm^{-1} . A vertical connecting the lowest point in the 1450 cm^{-1} trough was constructed intersecting the baseline. The percentage transmittance was recorded by registering the point where the vertical intersected the baseline and the minimum point of the trough. Similar procedures were used for the 1235 cm^{-1} band, employing approximately 1300 cm^{-1} and 1130 cm^{-1} as the baseline points.

The absorbance was calculated for each band utilizing:

$$\text{Absorbance} = \log_{10} (\text{baseline}) - \log_{10} (\text{trough})$$

Calculation of the helicity of the collagen sample was performed by determining the ratio of the absorbance obtained at 1235 cm^{-1} to that obtained at 1450 cm^{-1} . The resulting ratio was correlated to the percent helicity of the specimen utilizing the following linear relationship:

$$\text{Percent Helicity} = 119.05 (\text{Absorbance } 1235/1450) - 70.24$$

2.2.6 Transmission Electron Microscopy: Collagen Banding

The degree of banding of the collagen in the slurry was examined using transmission electron microscopy techniques outlined by Sylvester²⁰. Sylvester obtained the transmission electron photographs used in the determination of the banding of the experimental samples by use of a Philips EM300 transmission electron microscope (Philips NKV, Amsterdam).

The determination of banding was based on the degree of quaternary structure present in the collagen sample. Examination of the TEM photographs revealed collagen fibrils with varying quaternary structure. Forbes²¹ previously determined banding criteria utilizing a scale ranging from

0-4 encompassing the various fibril structures which were described by Sylvester as²⁰:

- 0 No Banding Visible
- 1 Slight Banding Visible
- 2 Banding Visible
- 3 Strong Banding Visible
- 4 Strong Banding with Intraperiod Banding Visible

Utilizing the banding criterion illustrated in Figure 2-5, all fibrils in the TEM photograph were measured and assigned a banding value. The fraction of fibrils with each degree of banding was determined using:

$$\beta_i = l_i/l_t$$

where:

$$\begin{aligned} \beta_i &= \text{fraction of fibrils with banding level } i \\ l_i &= \text{total length of fibrils with banding level } i \\ l_t &= \text{total length of all fibrils} \end{aligned}$$

The length average banding (LAB), representing the overall average banding in the photograph, was determined using:

$$\text{LAB} = \sum \beta_i(i)$$

where:

$$\begin{aligned} \beta &= \text{fraction of fibrils with banding level } i \\ i &= \text{banding level (0-4)} \end{aligned}$$

The results from the individual TEM photographs were averaged to determine an overall LAB for the collagen sample.

2.2.7 Scanning Electron Microscopy: Porosity

Examination of the porosity of the collagen matrix after freeze drying

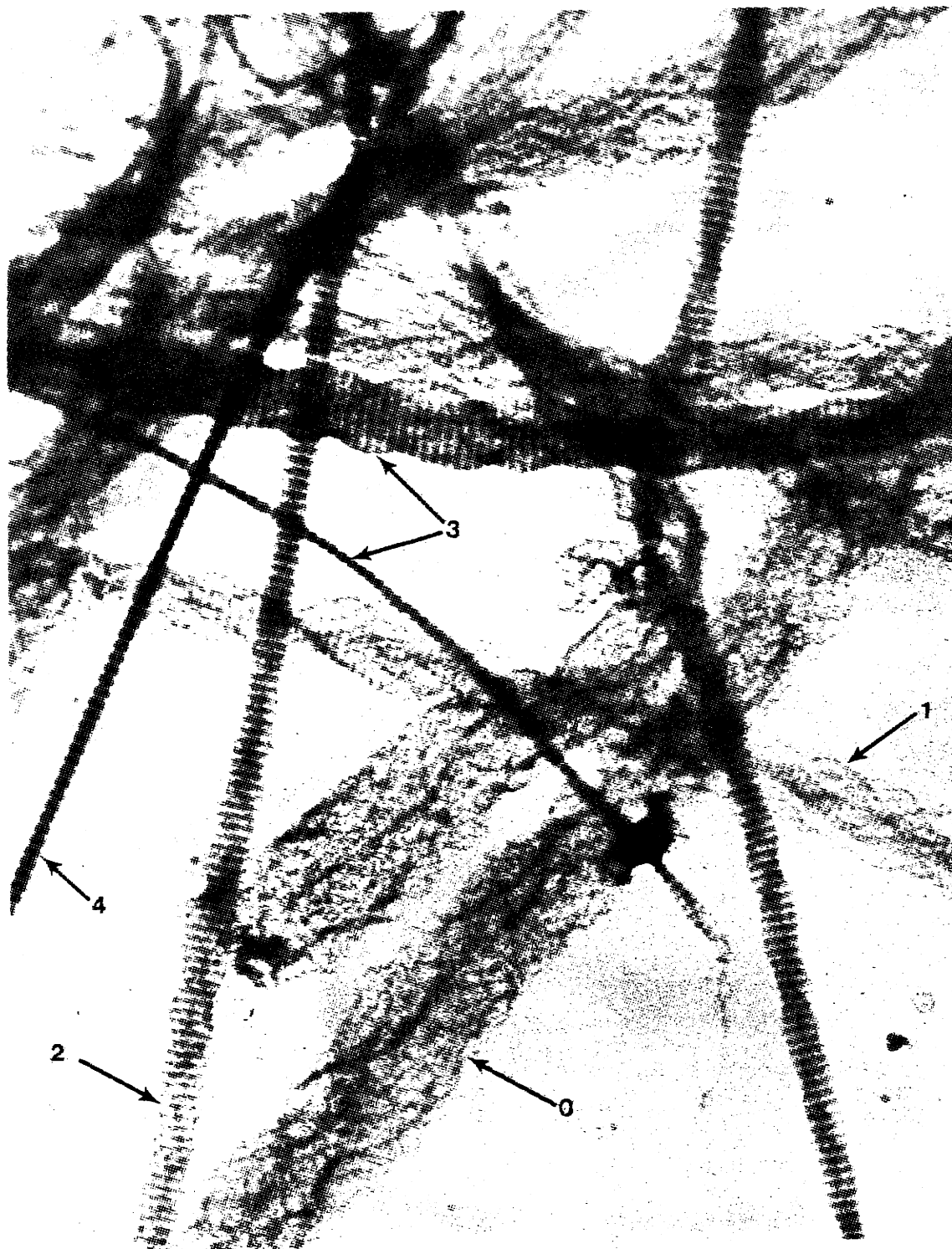


Figure 2-5: Collagen Banding Levels

and dehydrothermal treatment was performed utilizing a JOEL JSM U3 scanning electron microscope (JOELCO USA, Peabody, MA). Samples of representative pan sides (porous side) and cross sections were cut from the collagen foam utilizing a scapel. The sections were mounted on aluminum studs with silver paint and allowed to dry in the laminar air flow hood overnite.

Upon drying, the samples were coated with a layer of carbon followed by a thin layer of gold utilizing a vacuum evaporator (CVC vacuum evaporator, CVC Products, Rochester, N.Y.) The coated specimens were examined utilizing the SEM under an accelerating voltage of 20 KV. Photography of the collagen samples was performed at a standard magnification of 100x using Polaroid film (Type 52, Poloroid Corporation, Cambridge, MA).

The porosity of the collagen matrix was determined by obtaining a distribution of mean pore sizes from a collection of SEM photographs. This was performed by outlining the apparent upper layer of pores and obtaining a measure of each pore, as seen in Figure 2-6¹⁰. The values were averaged and a mean pore size determined for each SEM photograph. The various values from the photographs were averaged to obtain an overall average pore size.

2.2.8 M_c Testing: Crosslink Density

The crosslink density of the collagen membranes was determined following the protocol outlined by Yannas et al²². Briefly, a 3.0" by 1.0" sample of collagen-GAG membrane processed without siliconization was gelatinized in an 80°C physiological saline solution for a minimum of five minutes or until gelatinization was complete. The sample was next placed in the clamps of an

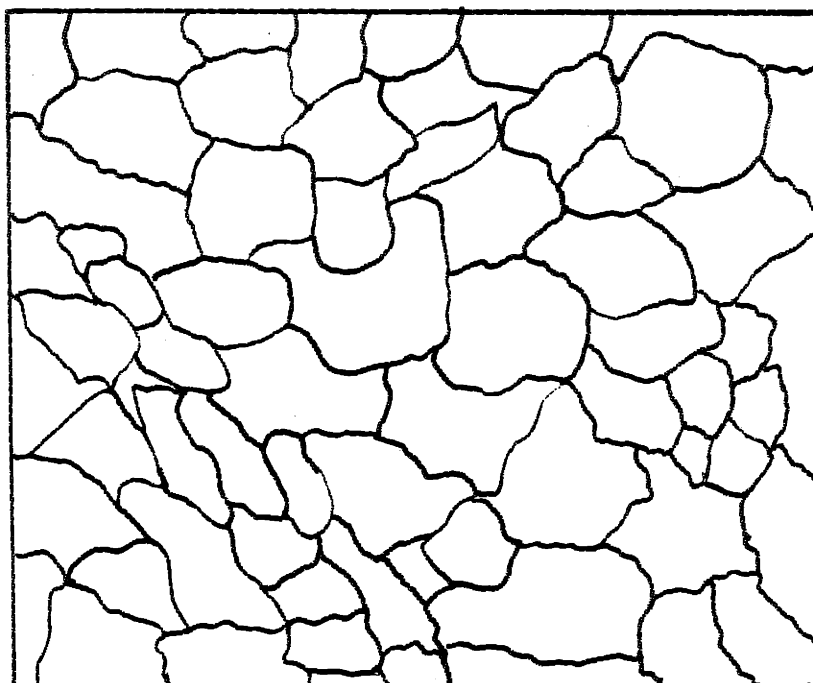
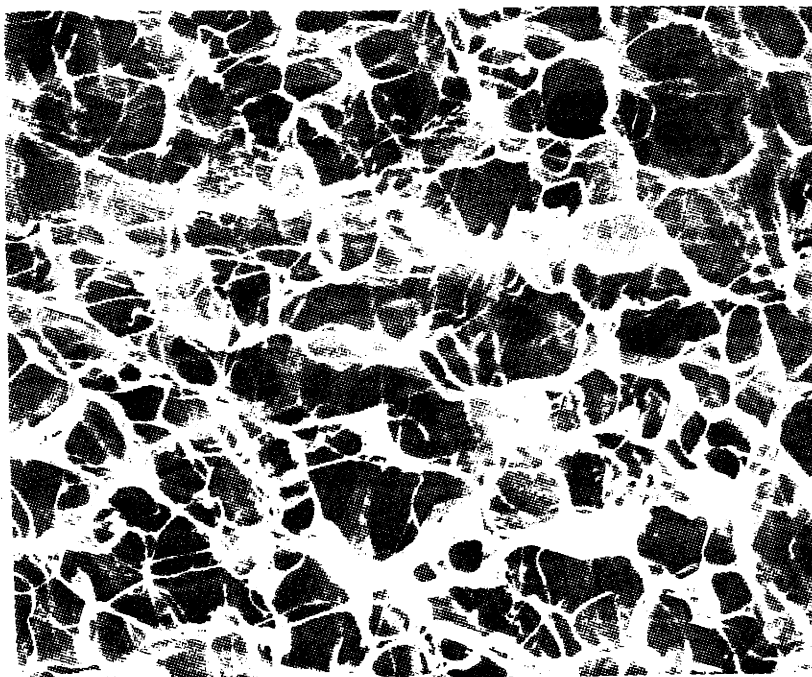


Figure 2-6: Determination of the Porosity of a Collagen Matrix.
Diagram of pore outline of photomicrograph.

Instron (Model TM table model tester with a 500g load cell, Instron Corporation, Canton, MA), immersed in 80°C physiological saline, and the Instron was manually extended 5% of its original length three times, allowing a minimum of five minutes between extensions for the sample to reach its asymptotic limit of strain. After removal from the clamps, the ends compressed by the Instron grips were removed. The width and thickness of the gelatinized collagen sample were measured. A dry weight of the sample was taken by analytically weighing the sample before and after twenty four hour drying in a 105°C oven.

M_c is a reciprocal measure of crosslink density. Upon gelatinization, the collagen foam can be modeled as an ideal rubber and the following equation used to determine the M_c value²².

$$\sigma = (\rho RT/M_c) (V_2)^{1/3} (\alpha - 1/\alpha^2)$$

where:

- σ = force on specimen divided by cross sectional area of swollen, unstretched specimen
- α = stretched specimen length divided by unstretched specimen length
- V_2 = volume fraction of polymer
- ρ = density of dry polymer
- T = absolute temperature
- R = universal gas constant
- M_c = average molecular weight between crosslinks

2.2.9 $1/\tau$ Testing: Collagenase Degradation

The collagenase degradation rates of the collagen membranes were determined following a modification of the in vitro technique originally described by Huang¹². The collagenase degradation rates for the experimental foams were determined by Wilson utilizing $1/\tau$ testing techniques¹³.

2.2.10 Hexosamine Assay: Percent GAG

To determine the glycosaminoglycan content of the collagen membrane following processing, a hexosamine analysis was performed as described by Rubenstein¹⁷ following a refinement of the Elson-Morgan hexosamine assay¹⁸ performed by Swann and Balazs¹⁹.

A 1" by 1" sample of collagen membrane was processed through the original protocol without siliconization and stored in 70% isopropanol for one day. Upon rinsing with deionized water, the specimen was freeze dried for twenty four hours. The sample was analytically weighed after freeze drying.

The freeze dried membrane was placed in a 5 ml ampule (Wheaton Scientific, Millville, N.J.) and 1 ml of 6 M HCl (reagent grade, Ashland Chemical Co., Columbus, OH diluted with an equal volume of deionized water) added. The ampule was sealed under vacuum after removal of air to prevent the presence of oxygen by freezing and thawing the solution three times under vacuum. The mixture was allowed to undergo hydrolysis for four hours in a 95°C heating block (Temp-Blok Module Heater, Scientific Products, McGraw Park, IL) before the reaction was stopped by cooling under cold running water.

The contents were transferred to a clean test tube. Neutralization of the solution was performed by the addition of 1 ml of 6 N NaOH (pellets, Matheson, Coleman and Bell, Manufacturing Chemists, Norwood, OH dissolved in deionized water).

Estimating an original glycosaminoglycan content of 880 $\mu\text{g}/\text{in}^2$ in the sample foam, the hydrolyzate was diluted to fall in the concentration range of 10-120 $\mu\text{g}/\text{ml}$ by the addition of deionized water. 1 ml of the hydrolyzate was placed in a clean test tube. Upon addition of 1 ml of fresh acetylacetate

reagent (reagent grade, Fisher Scientific Corp., Fair Lawn, N.J.), the test tube was placed in a 95°C water bath (LabLine Instruments, Inc., Melrose Park, IL) for one hour. Acetylacetate reagent was prepared immediately prior to use by mixing 2 ml of acetyl acetone (reagent grade, Fisher Scientific corp., Fair Lawn, N.J.) with 23 ml of 1 M sodium carbonate (certified, Fisher Scientific Corp., Fair Lawn, N.J.).

After stopping the reaction by cooling under cold running water, 5 ml of isopropanol were added. 1 ml of Ehrlich's reagent was next added and the tube inverted several times. Ehrlich's reagent was prepared by dissolving 1.33 g p-dimethylaminobenzaldehyde (certified, Fisher Scientific Corp., Fair Lawn, N.J.) in 50 ml 6 M HCl and adding 50 ml of isopropanol. The tube was stored at 4°C for two hours to permit colorimetric development.

The absorbance of the sample was examined at 527 nm with a Colman Junior IIA Linear Absorbance Spectrophotometer (Colman Instruments, Maywood, IL). The resultant value was compared to a standard calibration curve developed during the experiment using similar procedures to obtain a value of glycosaminoglycan content.

2.2.11 *In Vivo* Response

Two facets of the *in vivo* response to the collagen membrane were examined: wound contraction and cellular infiltration. Techniques similar to those developed by Chen¹⁰ were used in the *in vivo* studies.

Female white Hartley guinea pigs (Charles River Animal Suppliers, Wilmington, MA) were prepared for surgery by removal of the dorsal hair utilizing clippers (Oster Model AS-small, Oster Professional Products,

Milwaukee, WI) followed by treatment with a depilatory (Nair, Carter-Wallace, Inc., New York, N.Y.). The surgical area of the animal was cleansed prior to surgery by repeated scrubbing with betadiene (The Purdue Frederick Company, Norwalk, CT), followed by washing with 70% isopropanol.

The animal was anesthetized by inhalation of 0-80% nitrous oxygen and 0-3% halothane with oxygen (Vetaflex 5 Veterinary Anesthesia Machine, Pittman Moore). 3 cc of keflin (Cephalothin Sodium for Injection, Eli Lilly & Co., Indianapolis, IN) were injected intramuscularly in the hindquarter to serve as an antibiotic.

A 3.0 cm by 1.5 cm area of skin was surgically excised down to, but excluding, the panniculus carnosus. The halothane setting was reduced and the woundbed allowed to attain hemostasis. A 3.0 cm by 1.5 cm siliconized membrane was grafted in the woundbed silicone side up utilizing ten sutures (5-0 Ethilon Monofilament Nylon, Ethicon, Inc., Somerville, N.J.).

After photographing the graft with a 35 mm camera (Nikon camera with Micro Nikkor 55 mm lens, Japan using Kodachrome 64 film, Eastman Kodak Company, Rochester, New York), a sterile gauze (Topper dressing sponges, Johnson and Johnson Products, Inc., New Brunswick, N.J.) was placed on the wound surface. The animal was bandaged with two elastoplast bandages (Elastoplast, Beiersdorf Inc., South Norwalk, CT with topper dressing sponge) to protect the graft from damage.

The wound was examined at three or four day intervals to detect infection, to determine the adhesion of the graft to the wound surface, and to study contraction. The graft was photographed at each interval. Before rebandaging, the graft was treated with neosporin ointment (Burroughs

Wellcome Co., Research Triangle Park, N.C.) about the wound edges.

The contraction of the skin wound was numerically represented by the percent wound area remaining open. This was obtained by dividing the area of the wound remaining open by the original wound area (4.5 cm^2). The wound area remaining open was determined by measuring the pink area of the graft surrounded by the whitish epidermal ingrowth as seen in Figure 2-7. The length and width were determined by direct measurement of the graft on the animal, utilizing average values over the graft which contracted as a rectangle. As the contraction could clearly be seen beneath the silicone layer, removal of the silicone was not necessary.

Data on the cellular infiltration of the grafted woundbed was obtained from histological slides prepared from excised guinea pig grafts. Guinea pigs were sacrificed on Days 7, 14, 21, and 28 utilizing a 1 cc injection of Somlethol (sodium pentobarbital solution, J.A. Webster, Inc., North Billerica, MA). The grafts were surgically excised through all the skin layers, including the panniculus carnosus, and stored in formalin (10% v/v solution, neutralized phosphate buffered, J.T. Baker Chemical Co., Phillipsburg, N.J.) for at least twenty four hours. Cross sections and longitudinal sections were taken from the grafts, placed in specimen holders, and stored in formalin. Histological slides were prepared by the Angell Memorial Division of the Massachusetts S.P.C.A. from the sectioned grafts.

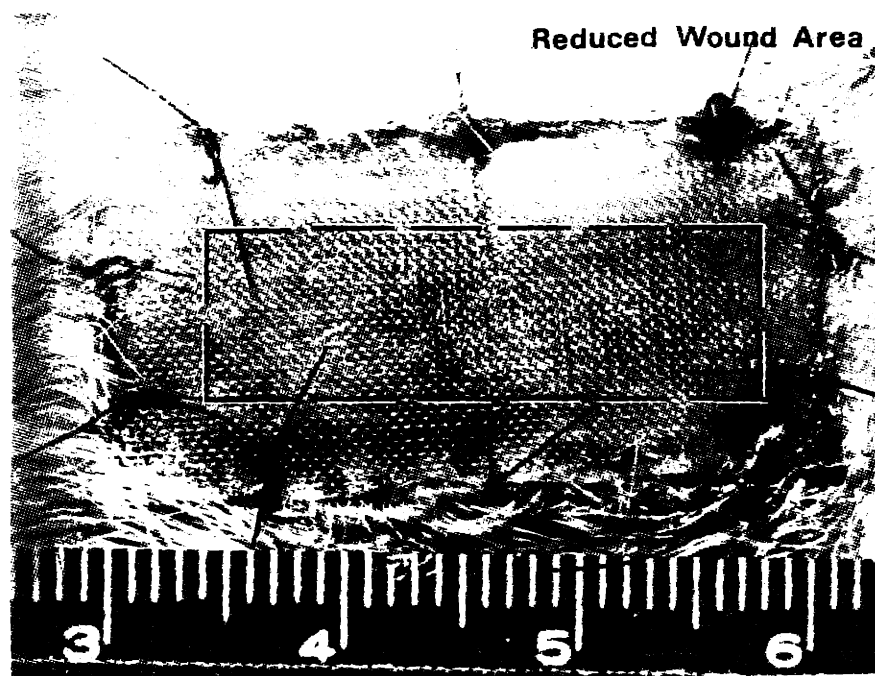
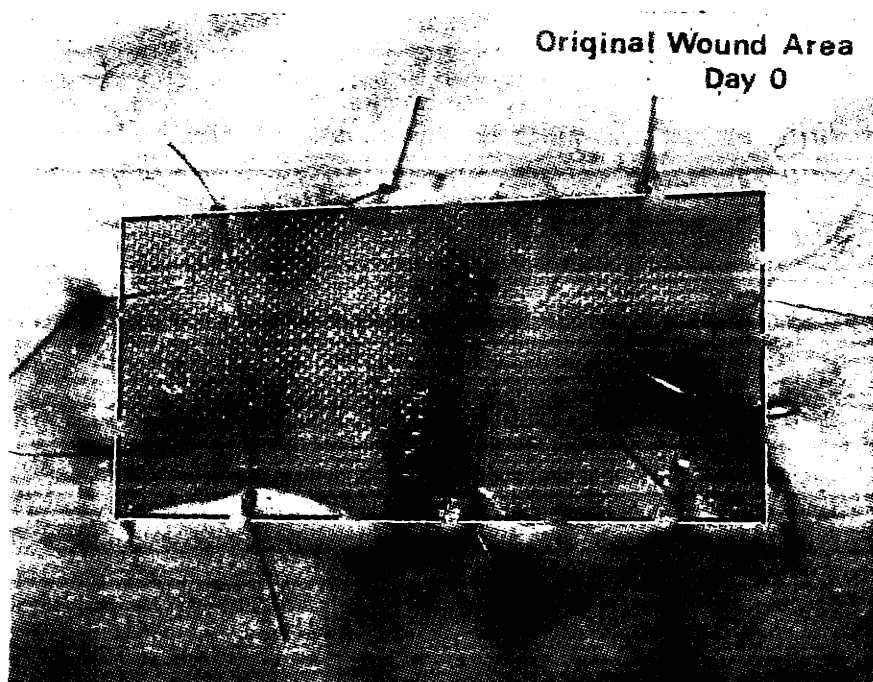


Figure 2-7: Measurement of Wound Contraction Exhibited by Grafted Woundbed.
Comparison of wound area at Day 0 to contracted wound.

Chapter 3

Results

3.1 Percent Solids

As seen in Table 3-I, the percent solids of the control GAG slurry prior to freeze drying is greater than that of the No GAG slurries. There is expected to be a .05% reduction in the percent solids of the No GAG slurries due to the lack of glycosaminoglycan, as the glycosaminoglycan is approximately 8% of the solids content. The additional difference in percent solids may be explained by the formation of high density collagen pellet during centrifugation of the No GAG slurries. The high density pellet was not utilized during slurry reblending due to its high concentration of particulate matter and its percent solids not determined.

Table 3-I: Percent Solids

| Foam Number | Trials | Slurry Type | Slurry | Supernatant |
|-------------|--------|-------------|----------|-------------|
| 82063 | 3 | GAG | .51±.01% | .00±.01% |
| 82066 | 3 | No GAG | .32±.05% | .00±.01% |
| 83009 | 3 | No GAG | .34±.07% | .00±.01% |

3.2 Collagen Helicity

The collagen helicities of the two slurries seen in Table 3-II indicate the GAG and No GAG slurries both exhibit high degrees of helicity. The difference seen in the helicities may be due to the influence of the glycosaminoglycan on either the 1450 cm^{-1} band or the 1235 cm^{-1} band.

Table 3-II: Collagen Helicity

| Foam Number | Trials | Slurry Type | Helicity |
|-------------|--------|-------------|--------------------|
| 82063 | 4 | GAG | $95.41 \pm 8.69\%$ |
| 82066 | 4 | No GAG | $78.53 \pm 5.73\%$ |

3.3 Collagen Banding

As indicated in Table 3-III, the GAG and No GAG slurries exhibit relatively little banding. The GAG slurry depicted in Figure 3-1 was calculated to have a length average banding (LAB) of 1.26. The GAG banding is double the length average banding of .60 determined for the No GAG slurry seen in Figure 3-2. This may be due to the interaction of the GAG preventing some of the collagen from swelling at pH 3. However, both slurries demonstrate a quaternary structure which is relatively unbanded.

Table 3-III: Length Average Banding

| Slurry Type | Trials | LAB |
|-------------|--------|----------------|
| GAG | 4 | $1.25 \pm .15$ |
| No GAG | 4 | $.60 \pm .31$ |



Figure 3-1: TEM Photomicrograph of Collagen-GAG Slurry at pH 3



Figure 3-2: TEM Photomicrograph of Collagen-No GAG Slurry at pH 3

3.4 Porosity

The porosities estimated in Table 3-IV from the scanning electron photomicrographs indicate that the alteration in the shelf freezing temperature of the No GAG foams was able to induce a porosity similar to that of the control GAG foam. Both the cross section and porous side (pan side) of the control GAG foam are illustrated in Figure 3-3. Figures 3-4 and 3-5 depict the cross sections and porous sides of the two No GAG foams prepared. Although the No GAG foams exhibit similar pore sizes to the control GAG foam, the No GAG foams contain channeling which is not seen in the control foam. The channeling is evident in both the cross sectional and pan side views.

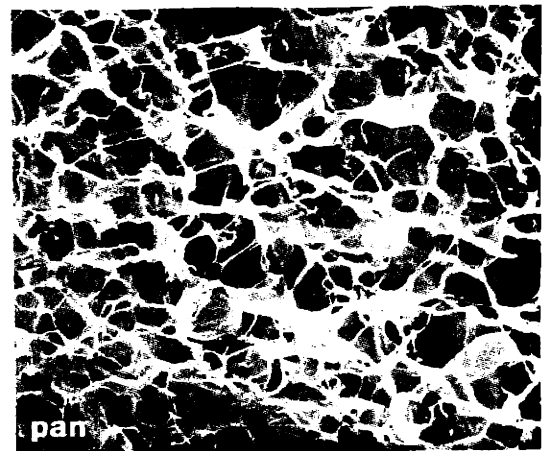
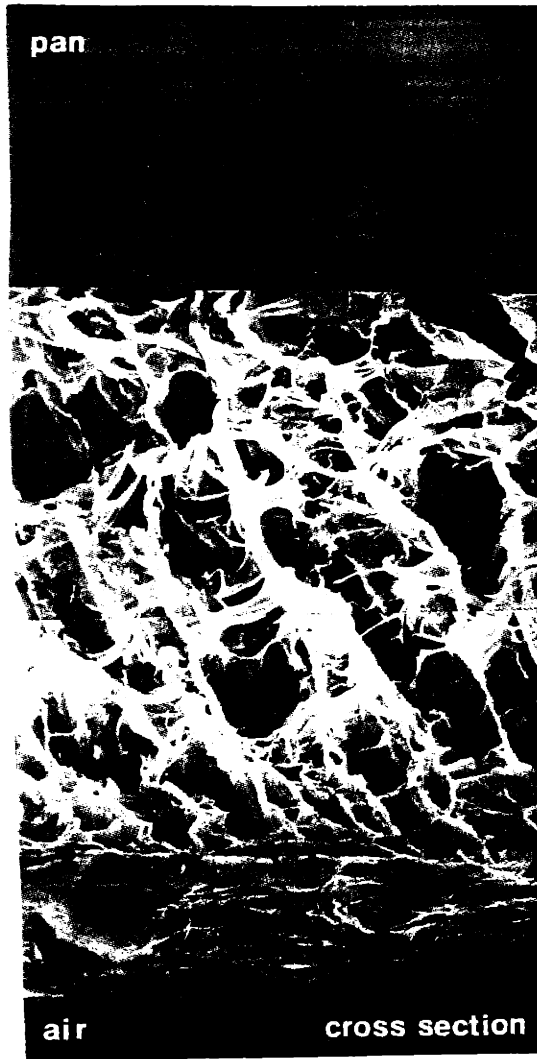
Table 3-IV: Porosity

| Foam Number | Trials | Foam Type | Mean Porosity(μm) | Shelf Temperature($^{\circ}\text{C}$) |
|-------------|--------|-----------|--------------------------------|---|
| 82063 | 3 | GAG | 150 \pm 10 | -40 |
| 82066 | 3 | No GAG | 160 \pm 26 | -20 |
| 83009 | 3 | No GAG | 163 \pm 15 | -20 |

3.5 Crosslink Density

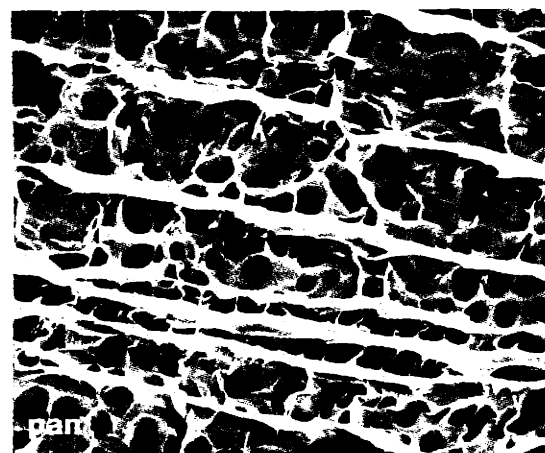
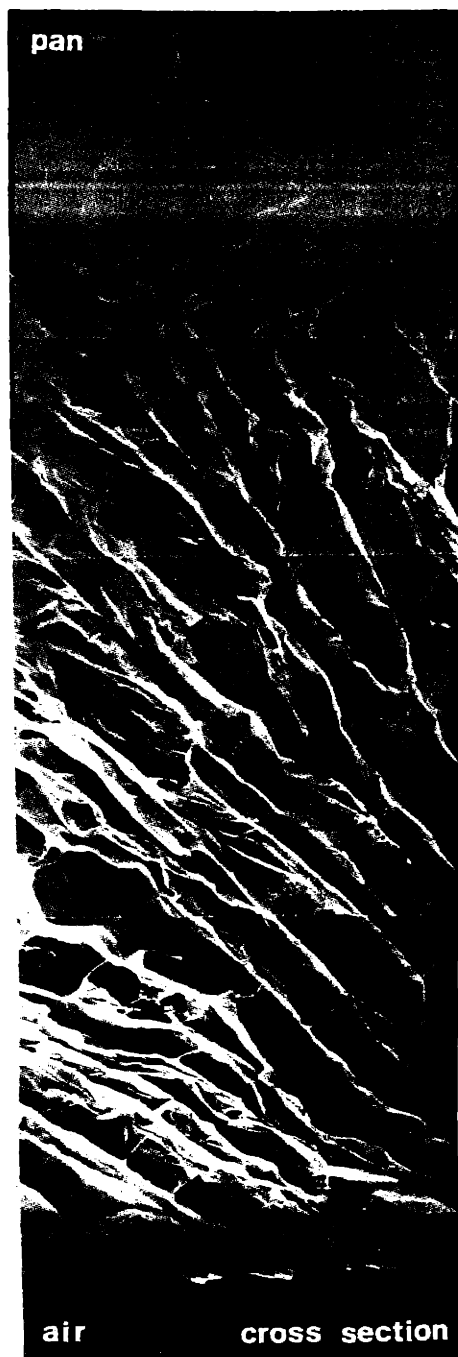
As illustrated in Table 3-V, the deletion of crosslinking with .25% glutaraldehyde during processing induced a significant reduction in the number of crosslinks. This is represented by the 40,000 daltons found between crosslinks in the No GAG, uncrosslinked foam as compared to both the 9500 daltons between crosslinks found in the GAG, crosslinked foam and the 12,000

Figure 3-3: SEM Photomicrographs of Control GAG, Crosslinked Membranes



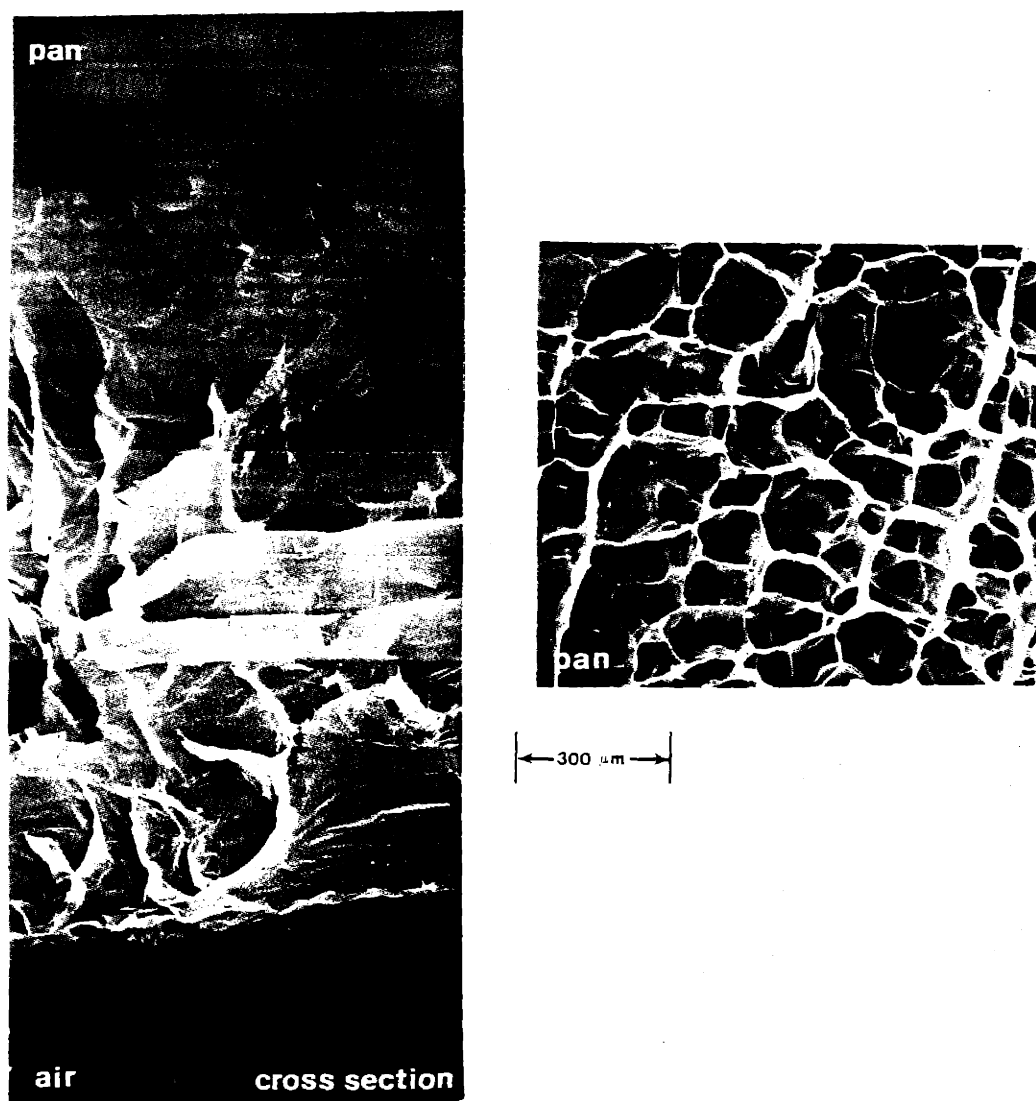
300 μ m

Figure 3-4: SEM Photomicrographs of No GAG, Crosslinked Membranes



300 μ m

Figure 3-5: SEM Photomicrographs of No GAG, Uncrosslinked Membranes



daltons between crosslinks in the No GAG, crosslinked foam.

The presence of GAG in the collagen matrix does not significantly alter the crosslink density. Both the GAG, crosslinked membrane and the No GAG, crosslinked membrane demonstrated crosslink densities within error of one another. This indicates no significant difference in crosslink density between the two.

Table 3-V: Crosslink Density

| Foam Number | Trials | Membrane Type | M_c Value |
|-------------|--------|-----------------------|---------------------|
| 82063 | 4 | GAG, Crosslinked | $9,500 \pm 4,000$ |
| 82066 | 6 | No GAG, Crosslinked | $12,000 \pm 6,000$ |
| 83009 | 4 | No GAG, Uncrosslinked | $44,000 \pm 28,000$ |

3.6 Collagenase Degradation

Wilson, for various samples described in this work,, experimentally determined the $1/\tau$ values seen in Table 3-VI¹³. The values indicate the presence of GAG in the membrane decreases the collagenase degradation rate. The values listed were normalized by correcting a standard sample run daily to a $1/\tau$ equaling $15.0 \times 10^{-3} \text{ min}^{-1}$. This corrected for daily variations in the collagenase activity. The decrease of the collagenase degradation rate with the addition of glycosaminoglycan was positive only in the positive strain region¹³.

Table 3-VI: Collagenase Degradation

| % Strain | 1/ τ Values ($1 \times 10^{-3} \text{ min}^{-1}$) | | | |
|----------|--|--------|---------------------|--------|
| | GAG, Crosslinked | Trials | No GAG, Crosslinked | Trials |
| 10 | 6.5 \pm 7.1 | 9 | 12.5 \pm 11.4 | 10 |
| 13 | 6.1 \pm 3.0 | 9 | 21.9 \pm 15.9 | 10 |
| 16 | 8.3 \pm 4.6 | 8 | 36.9 \pm 11.2 | 10 |
| 19 | 9.2 \pm 4.1 | 7 | 30.9 \pm 22.3 | 10 |
| 22 | 8.5 \pm 4.2 | 7 | 43.5 \pm 26.1 | 8 |

3.7 Percent GAG

Table 3-VII indicates the percent glycosaminoglycan content calculated utilizing a hexosamine assay for the various foams. The slurries which contained 8% w/w chondroitin-6-sulfate before freeze drying were found to retain 3% w/w chondroitin-6-sulfate upon completion of wet processing. This indicates the loss of some glycosaminoglycan due to elution during the wet processing; including soaking in acetic acid (0.05 M, pH 3), .25% glutaraldehyde (pH 3), deionized water, and 70% isopropanol. Foams processed from slurries which had no addition of chondroitin-6-sulfate exhibited a minimal 0.35% glycosaminoglycan content. This calculated figure could represent either background noise in the spectrophotometer or a minimal concentration of glycosaminoglycan found in the collagen.

The data also indicates that the lack of glutaraldehyde crosslinking does not significantly affect the amount of glycosaminoglycan eluted during wet processing. This suggests that an uncrosslinked membrane should not differ from a crosslinked membrane in glycosaminoglycan content.

During the hexosamine assay, it was noted that the samples without glutaraldehyde crosslinking dissolved in the 6 M HCl during vacuum evacuation. However, the samples which were crosslinked with glutaraldehyde required ten minutes in the 95°C heating block before completely dissolving.

Table 3-VII: Glycosaminoglycan Content

| Foam Number | Type | Percent Glycosaminoglycan Content | Trials |
|-------------|-----------------------|-----------------------------------|--------|
| 82089 | No GAG, Uncrosslinked | 0.35% | 1 |
| 82089 | No GAG, Crosslinked | 0.35% | 1 |
| 82054A | GAG, Uncrosslinked | 3.01% | 1 |
| 82054A | GAG, Crosslinked | 2.67% | 1 |

3.8 Histology: Cellular Infiltration

Histological specimens were prepared from grafts taken on days 7, 14, 21, and 28 as indicated in Table 3-VIII. Interpretations of the individual histologies utilizing light microscopy are outlined in Tables 3-IX, 3-X, and 3-XI.

The GAG, crosslinked grafts provided a surface over which epithelial cells migrated, covering 25% of the graft by day 14 as seen in Figure 3-6. As illustrated in Figure 3-7, epithelialization was complete by day 28. As early as day 14, the matrix permitted both vascularization and cellular infiltration. By day 14, the cellular infiltration consisted of fibroblasts aligning over the panniculus carnosus in the bottom of the matrix, multinucleated giant cells digesting collagen in the center of the matrix, and lymphocytes and macrophages brought in through the newly formed capillaries. Between days 14 and 28, the fibroblasts began to travel into the matrix and divide while the

Table 3-VIII: Animal Study Data

| Animal No. | Type of Graft | Silicone Ejection | Infection | Sacrifice |
|------------|--------------------|-------------------|-----------|-----------|
| S-10 | GAG,Crosslinked | Peeling on Day 21 | Yes | Day 21 |
| | No GAG,Crosslinked | Peeling on Day 21 | No | Day 21 |
| S-11 | GAG,Crosslinked | Day 21 | No | Day 28 |
| | No GAG,Crosslinked | Day 21 | No | Day 28 |
| S-12 | GAG,Crosslinked | Adhered on Day 14 | No | Day 14 |
| | No GAG,Crosslinked | Adhered on Day 14 | No | Day 14 |
| S-13 | GAG,Crosslinked | Adhered on Day 7 | No | Day 7 |
| | No GAG,Crosslinked | Adhered on Day 7 | No | Day 7 |
| S-14 | GAG,Crosslinked | Day 46 | No | Day 153 |
| | No GAG,Crosslinked | Day 21 | No | Day 153 |
| S-15 | GAG,Crosslinked | Day 33 | No | Long Term |
| | No GAG,Crosslinked | Day 21 | No | Long Term |

Figure 3-VIII, continued

| Animal No. | Type of Graft | Silicone Ejection | Infection | Sacrifice |
|----------------------|---|---|-----------|-----------|
| S-50 thru S-56 | GAG,Crosslinked No GAG,Uncrosslinked | One animal died on Day 1, five animals died on Day 2, one animal died on day 4. Autopsy performed. Cause of death unknown, possibly linked to pneumonia prior to surgery. | | |
| S-60 | No GAG,Uncrosslinked | Day 14 | No | Day 14 |
| S-61 | No GAG,Uncrosslinked | Adhered on Day 7 | No | Day 7 |
| S-62 | No GAG,Uncrosslinked | Day 25 | No | Long Term |
| S-63 | No GAG,Uncrosslinked | Day 25 | No | Day 28 |
| S-64 | No GAG,Uncrosslinked | Adhered on Day 7 | No | Day 8 |
| S-65 | No GAG,Uncrosslinked | Day 21 | No | Day 21 |
| S-66 | No GAG,Uncrosslinked | Day 16 | No | Long Term |
| S-67 | No GAG,Uncrosslinked | Died on Day 2 due to anesthesia | | |

Table 3-IX: Histological Findings - GAG, Crosslinked Membranes

| | |
|--------|--|
| Day 7 | No histology taken |
| Day 14 | Graft is well vascularized with capillary formation; 25% epithelial coverage over collagen matrix with hypercarotinosi at wound edges; fibroblasts present throughout matrix, aligning in plane over panniculus adiposus; multinucleated giant cells in matrix digesting collagen; presence of few eosinophils and neutrophils; infiltration of mononuclear cells; beginning of neodermal growth in bottom of matrix; some edema in graft. |
| Day 21 | Graft grossly infected |
| Day 28 | Well vascularized; complete epithelial coverage with keratin formation; fibroblasts present and dividing in the matrix; presence of fibrous connective tissue; large number of multinucleated giant cells; presence of moderate number of mononuclear cells; foci of hemorrhage in graft; complete neodermal generation at base of matrix; basal cells in base epithelium. |

Table 3-X: Histological Findings - No GAG, Crosslinked Membranes

| | |
|--------|--|
| Day 7 | No histology taken |
| Day 14 | Graft is fairly well vascularized with capillary formation; 25% epithelial coverage over collagen matrix with hypercarotinosiis at wound edges; fibroblasts present throughout the matrix; multinucleated giant cells in matrix digesting collagen; presence of a few eosinophils in center of graft; infiltration of mononuclear cells; some neodermal synthesis in bottom of matrix; edema near top of matrix. |
| Day 21 | Graft is fairly vascularized; complete epithelial coverage; presence of fibroblasts in matrix; multinucleated giant cells in matrix digesting collagen; presence of eosinophils and neutrophils near base of matrix; infiltration of mononuclear cells; neodermal synthesis at base of matrix. |
| Day 28 | Well vascularized; complete epithelial coverage; fibroblasts distributed throughout the graft; few multinucleated giant cells remaining in the matrix; few eosinophils and mononuclear cells in the collagen matrix; degradation of collagen matrix appears greater than that seen in the GAG, Crosslinked membrane; complete neodermal synthesis in base of graft; basil cells in base of epithelium. |

Table 3-XI: Histological Findings - No GAG, Uncrosslinked Membranes

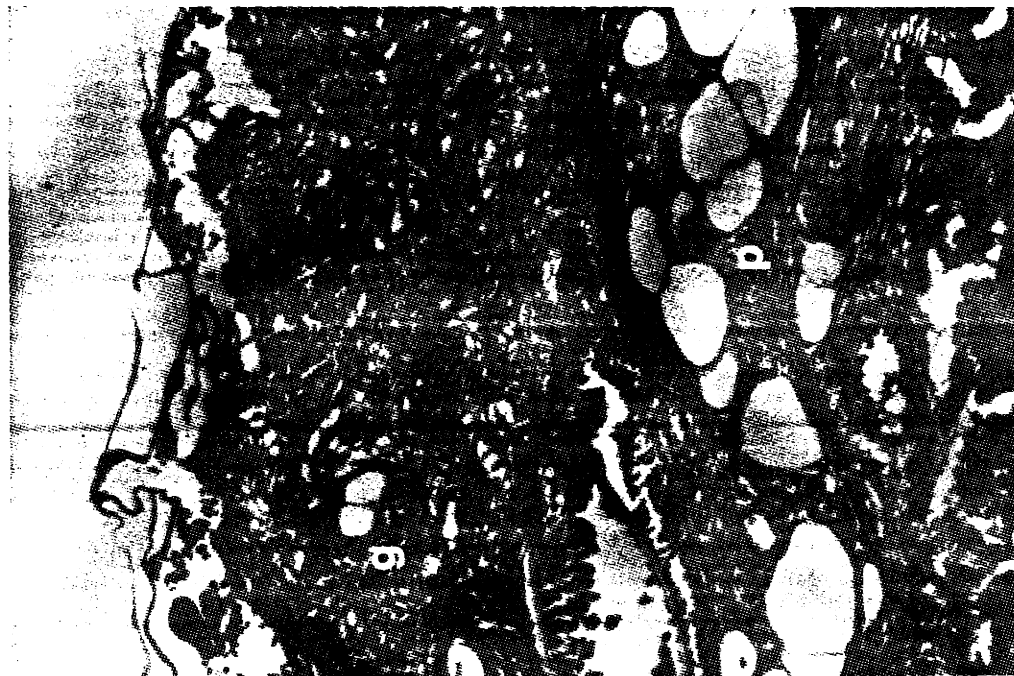
- Day 7 Graft not well vascularized; 20% epithelial coverage with hypercarotinosi at wound edges; few fibroblasts present in matrix; few multinucleated giant cells digesting collagen; infiltration of matrix by mononuclear cells; no apparent neodermal synthesis in bottom of matrix.
- Day 14 Graft not well vascularized; 100% epithelial coverage; large infiltration of fibroblasts in matrix; few multinucleated giant cells digesting collagen; little infiltration of matrix by mononuclear cells; little neodermal synthesis in base of membrane.
- Day 21 Graft partially vascularized; 80% epithelial coverage of matrix; infiltration of fibroblasts in matrix; many multinucleated giant cells digesting collagen; presence of some eosinophils in matrix; little neodermal synthesis in base of matrix.
- Day 28 Presence of capillary vessels in graft; 100% epithelial coverage; infiltration of fibroblasts in matrix; multinucleated giant cells digesting collagen; presence of eosinophils and some macrophages in the matrix; little neodermal synthesis in the base of matrix.



75x

Figure 3-6: Histological Sections: Control GAG, Crosslinked Membranes - Day 14
D=Dermis, E=Epidermis, G=Graft, P=Panniculus Adiposus

300x





75x

Figure 3-7: Histological Sections: Control GAG, Crosslinked Membranes - Day 28

D=Dermis, E=Epidermis, G=Graft, P=Panniculus Adiposus



300x

multinucleated giant cells continued to digest the collagen support. Simultaneously, the surrounding tissue was regenerating a neodermis in the bottom of the matrix, over the panniculus carnosus. The neodermal growth, begun by day 14, underlied the entire graft by day 28. Examination of the long term histology revealed an underlying bed consisting of a complete neodermis covered by a layer of fibroblasts. The wound was covered by epithelial cells in all stages of maturation.

The examination of the histologies of the No GAG, crosslinked grafts revealed a healing response similar to that of the GAG, crosslinked membranes. At day 14, there was 25% epithelialization with the presence of vascularization and neodermal formation in the graft, as demonstrated in Figure 3-8. However, the degradation of the collagen matrix by the multinucleated giant cells had progressed to a greater degree than that of the GAG, crosslinked matrix. Total epithelialization was seen by day 21. As seen in Figure 3-9, the generated neodermis covered the bottom of the matrix by day 28. Again, there was significantly less of the No GAG collagen matrix remaining at day 28 than the GAG collagen matrix. The woundbed present at long term consisted of a complete epithelial layer covering a layer of neodermis. Examination with 90° light polarization revealed the entire layer underlying the epidermis consisted of newly synthesized collagen.

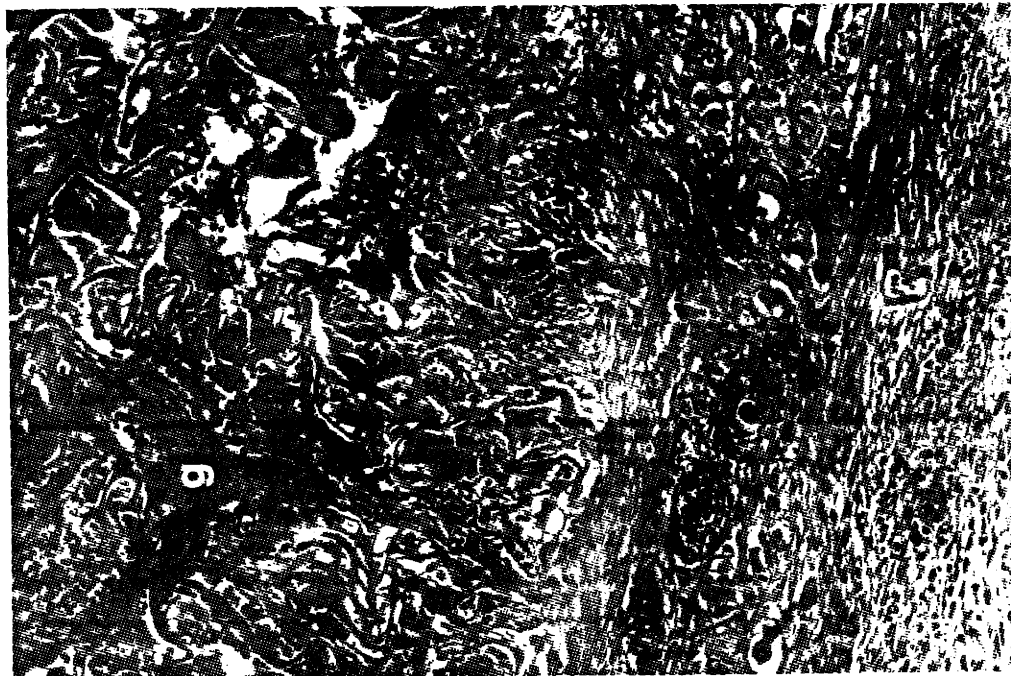
The sections from the No GAG, uncrosslinked membranes revealed 20% epithelial coverage by day 7 with complete epithelialization by day 14. Macrophages, along with few fibroblasts and multinucleated giant cells, were found in the matrix on day 7. As illustrated in Figure 3-10, the presence of fibroblasts dominated by day 14. Between days 14 and 28, the matrix was infiltrated by primarily fibroblasts with some macrophages and eosinophils as

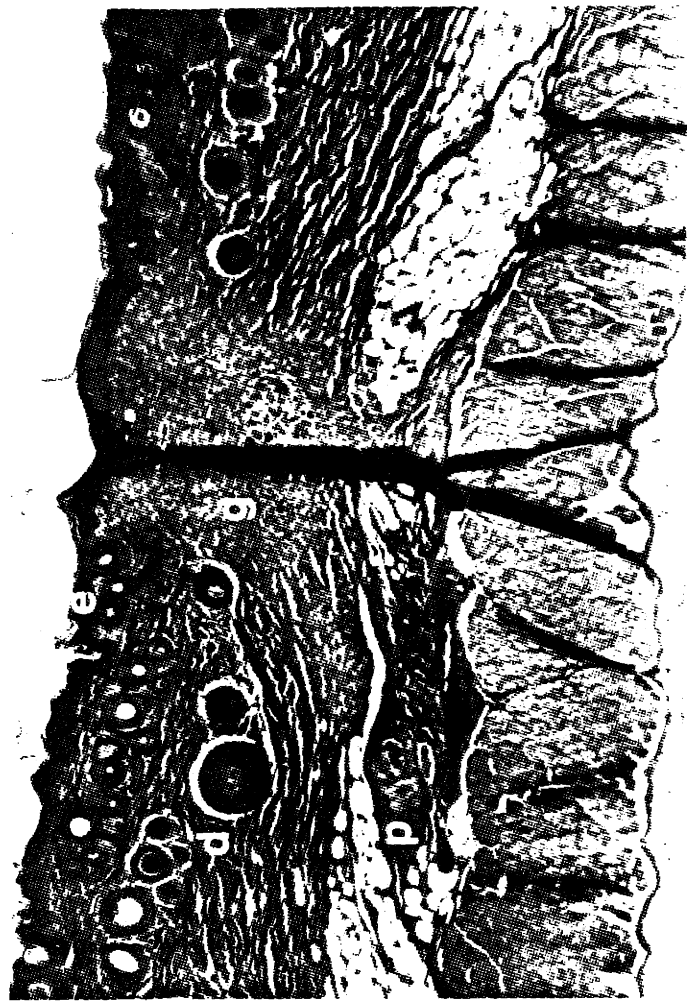


75x

Figure 3-8: Histological Sections: No GAG, Crosslinked Membranes - Day 14
D=Dermis, E=Epidermis, G=Graft, P=Panniculus Adiposus

300x





75x

Figure 3-9: Histological Sections: No GAG, Crosslinked Membranes - Day 28

D=Dermis, E=Epidermis, G=Graft, P=Panniculus Adiposus

300x





75x

Figure 3-10: Histological Sections: No GAG, Uncrosslinked Membranes - Day 14

D=Dermis, E=Epidermis, G=Graft, P=Panniculus Adiposus

300x



75x

Figure 3-11: Histological Sections: No GAG, Uncrosslinked Membranes - Day 28

D=Dermis, E=Epidermis, G=Graft, P=Panniculus Adiposus



300x

seen in Figures 3-10 and 3-11. Very little vascularization was seen between days 7 and 28, with the presence of few red blood cells in the membrane. Little infiltration of the bottom of the collagen matrix by generated neodermis progressed between days 7 and 28. It is noted that the tissue surrounding the wound pushed into the top of the collagen matrix by day 28 instead of the neodermis entering the bottom of the matrix.

3.9 Contraction/Epithelialization

Contraction of the woundbed was seen to be decreased by both the glutaraldehyde crosslinking of the membrane and the presence of chondroitin-6-sulfate in the matrix. Figures 3-12&3-13 illustrate the resultant contraction behavior of wounds treated with the No GAG, crosslinked membranes and the No GAG, uncrosslinked membranes respectively. Both are compared to the behavior demonstrated by an open wound and a wound treated with GAG, crosslinked artificial skin²³.

As seen in Figures 3-14 and 3-15, the onset of wound contraction/epithelialization was seen by day 14 for both the GAG, crosslinked foams and the No GAG, crosslinked foams. The contraction was seen to begin as early as day 5 for the No GAG, uncrosslinked foams, as illustrated in Figure 3-16.

Examination of the 50% wound closure point revealed a value of 19 days for the GAG, crosslinked foams. At day 16, the No GAG, crosslinked foams had reached 50% wound closure; increasing 50% wound closure by three days. The No GAG, uncrosslinked foams obtained 50% closure on day 12, increasing 50% wound closure by seven days.

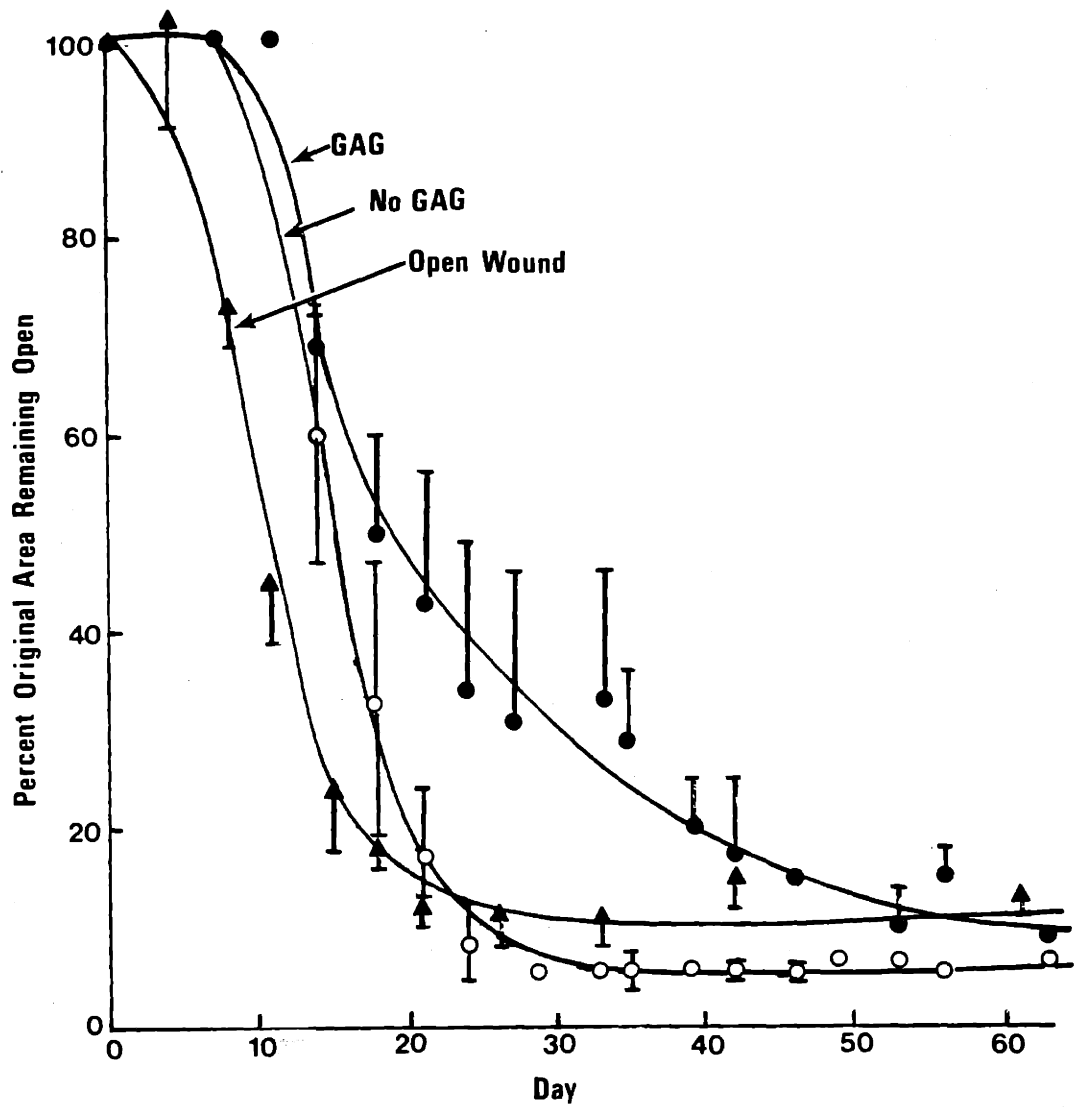


Figure 3-12: Composite of Wound Reduction Curves: Comparison of GAG, Crosslinked Membrane, No GAG, Crosslinked Membrane, and Untreated Wound

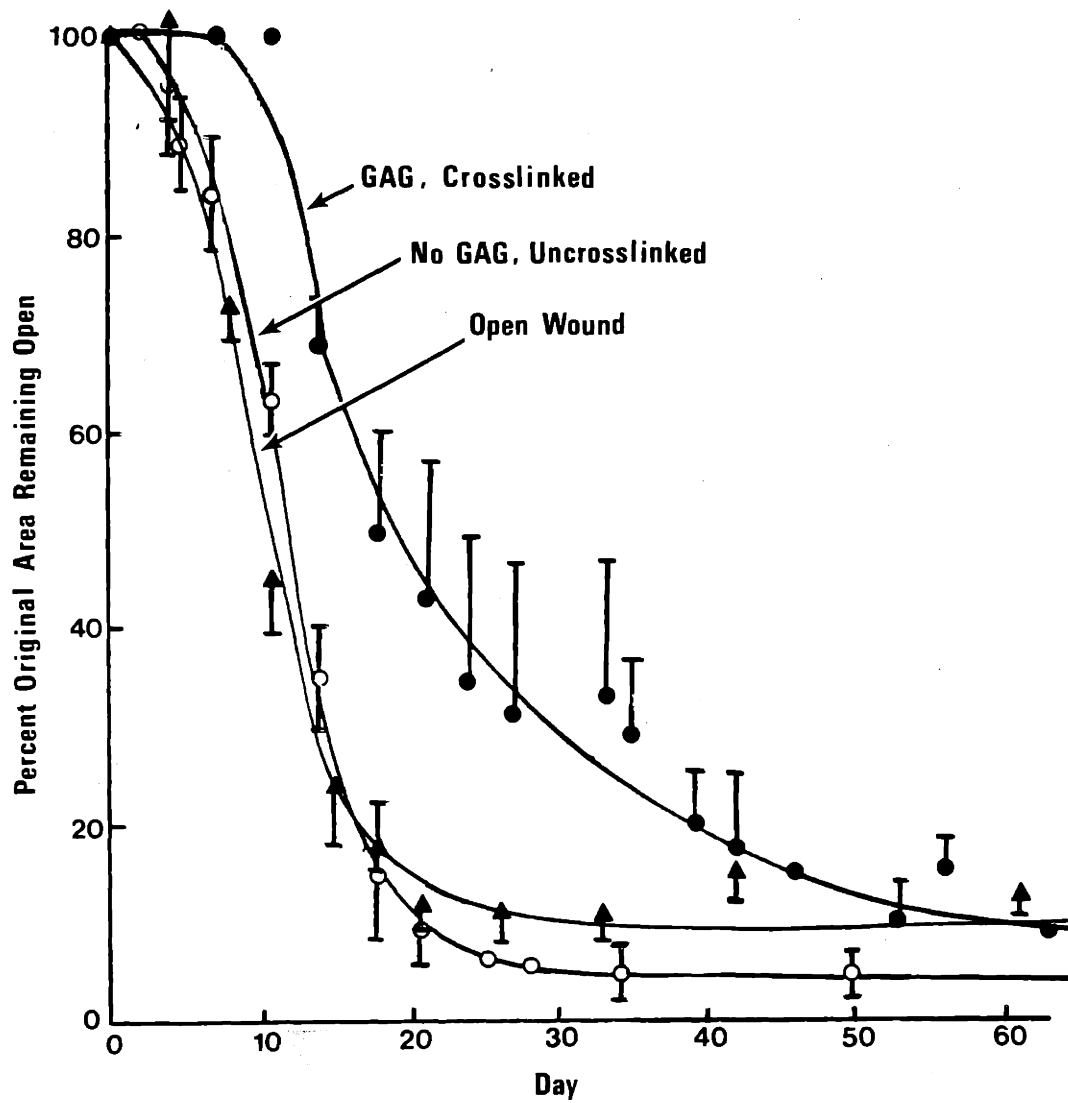


Figure 3-13: Composite of Wound Reduction Curves: Comparison of GAG, Crosslinked Membrane, No GAG, Uncrosslinked Membrane, and Untreated Wound

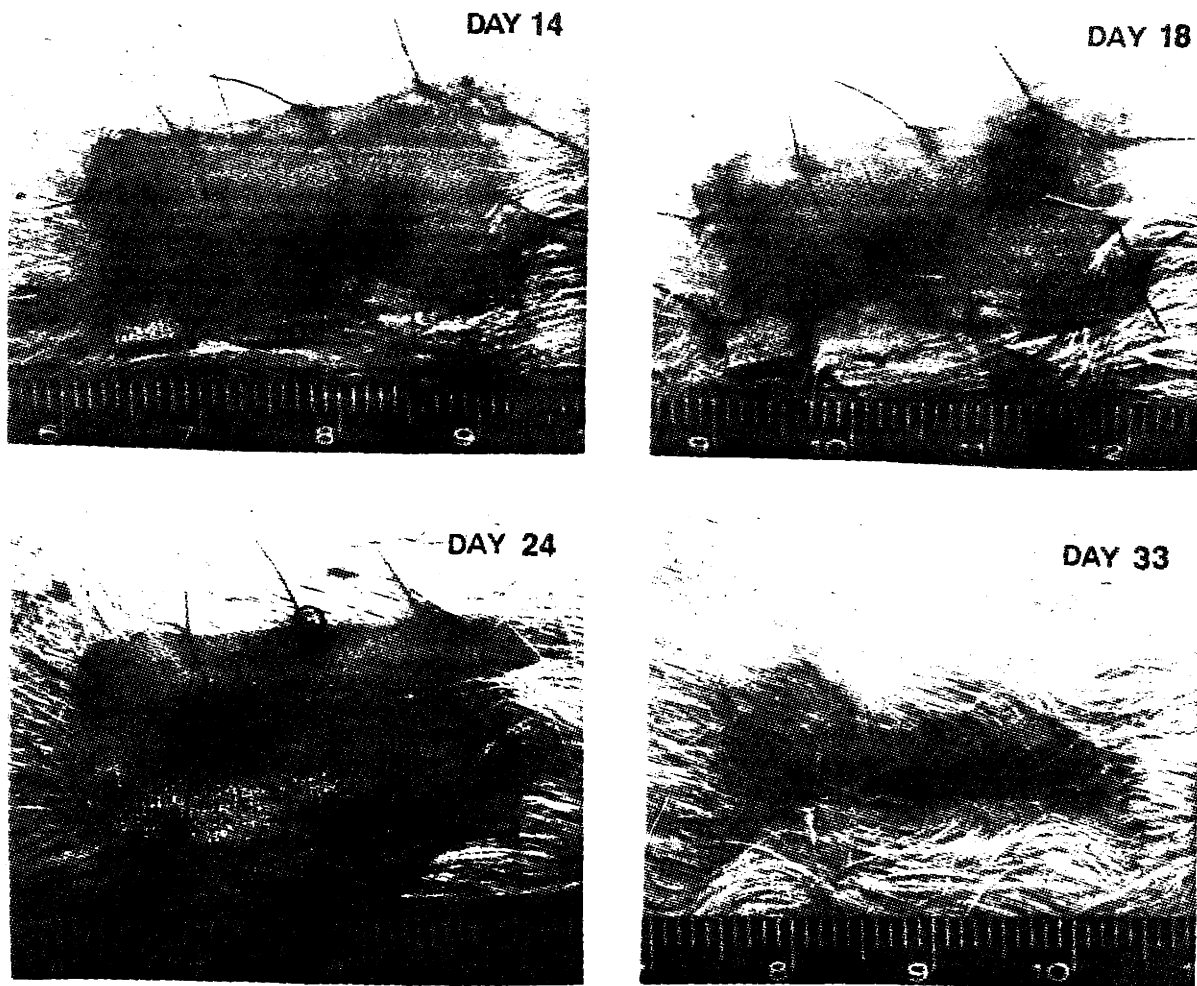


Figure 3-14: Wound Contraction of Control GAG, Crosslinked Membranes:
Days 14, 18, 24, and 33

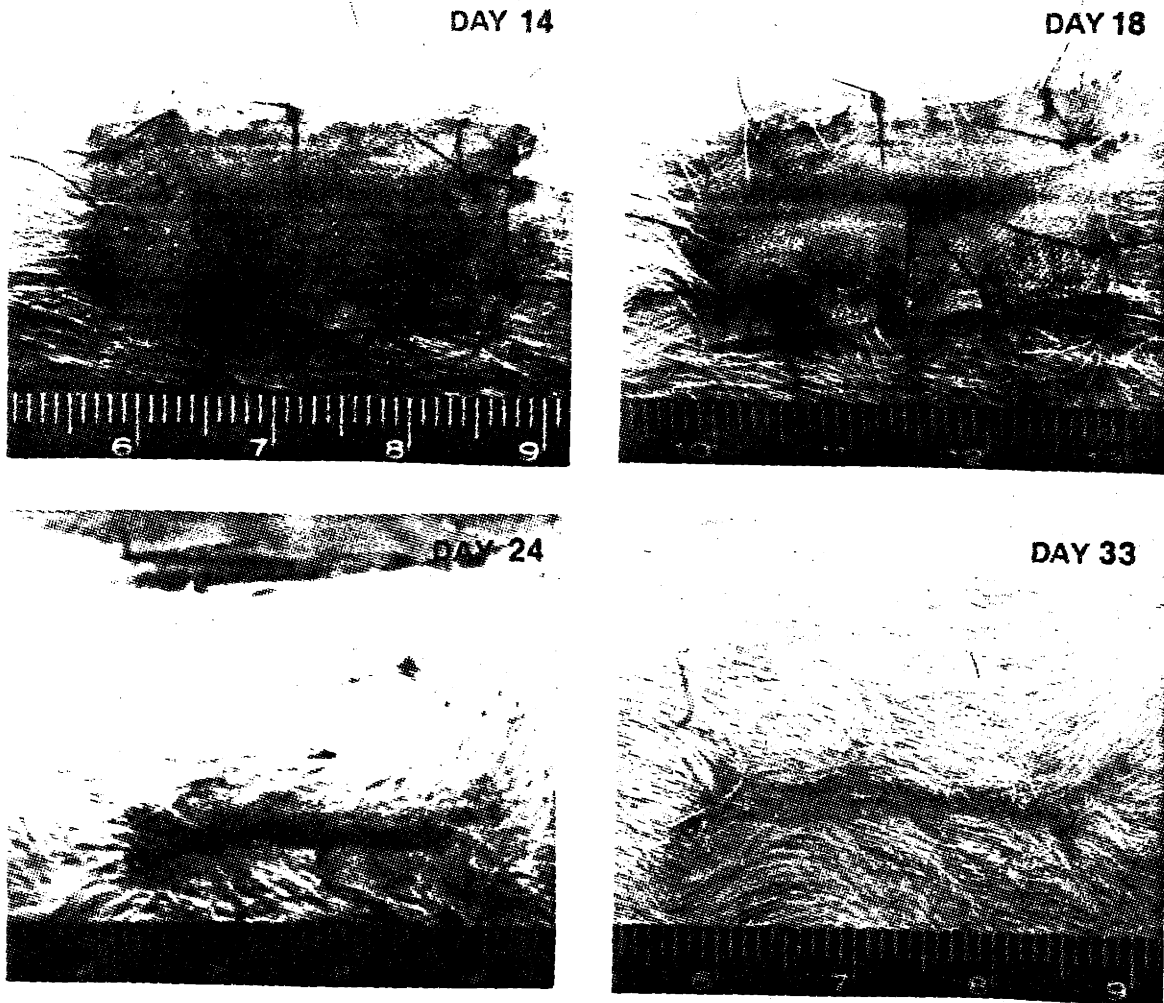


Figure 3-15: Wound Contraction of No GAG, Crosslinked Membranes:
Days 14, 18, 24, and 33

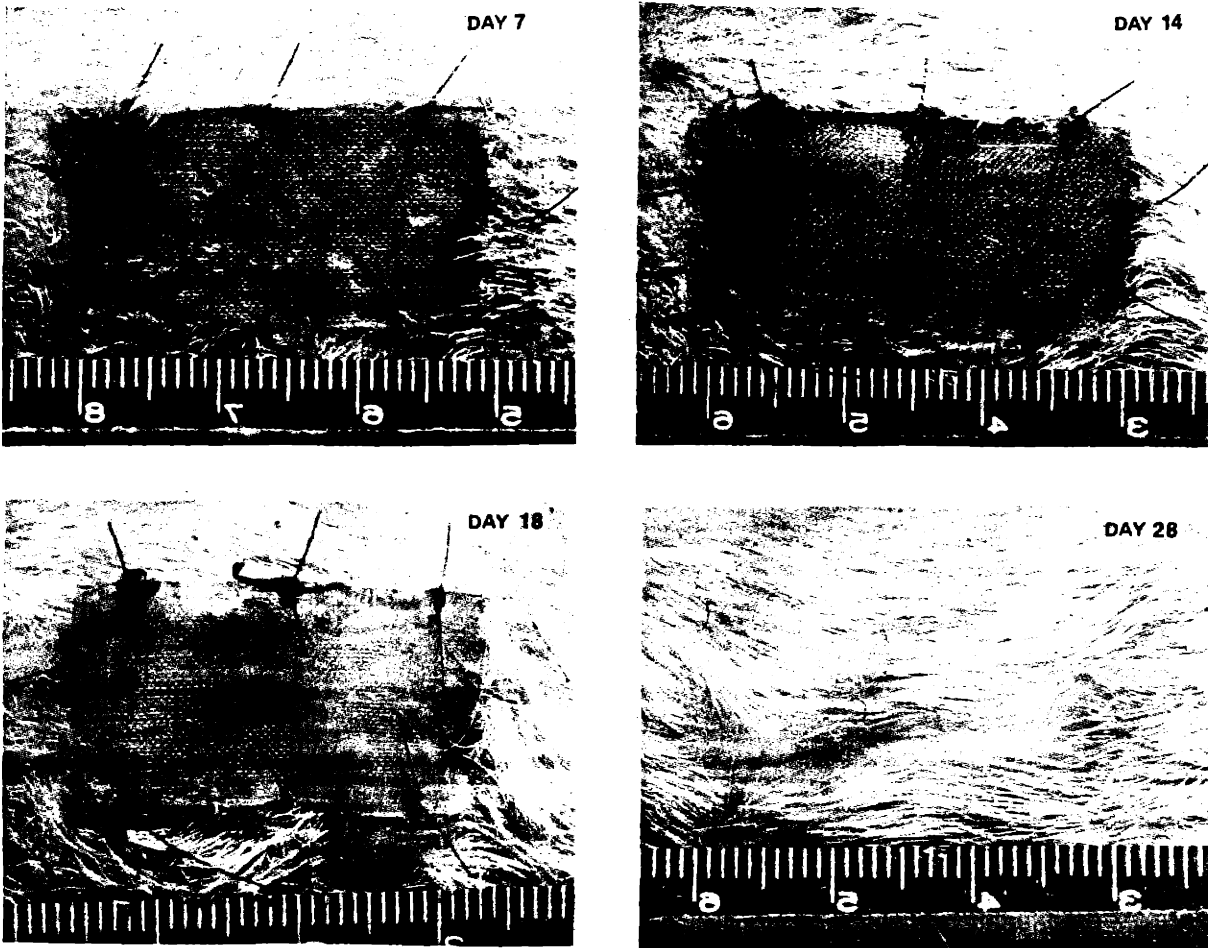


Figure 3-16: Wound Contraction of No GAG, Uncrosslinked Membranes:
Days 7, 14, 18, and 28

Silicone ejection occurred earlier for the No GAG, crosslinked and No GAG, uncrosslinked grafts than for the GAG, crosslinked grafts. As seen in Table 3-VIII, the silicone layer of the No GAG, crosslinked foam was ejected by Day 21 for all animals. The No GAG, uncrosslinked membranes ejected the silicone sheeting between Days 16 and 25. The silicone was found to remain on the GAG, crosslinked foams between 21 and 46 days.

A composite of the resultant contraction curves is illustrated in Figure 3-17. It was noted that the absence of GAG significantly increased the contraction of the woundbed during the later phases of contraction while the deletion of the membrane crosslinking in .25% glutaraldehyde increased the contraction during the earlier phases.

Linear regressions were performed on the contraction data between approximately Day 4 and Day 24. The results are listed in Table 3-XII. The -5.6% wound area/day closure of the No GAG, crosslinked membrane and -5.9% wound area/day closure of the No GAG, uncrosslinked membranes are greater than the value of -3.9% demonstrated by the control GAG, crosslinked membranes. This indicated the lack of glycosaminoglycan and glutaraldehyde crosslinking increased the contraction rate of the woundbed.

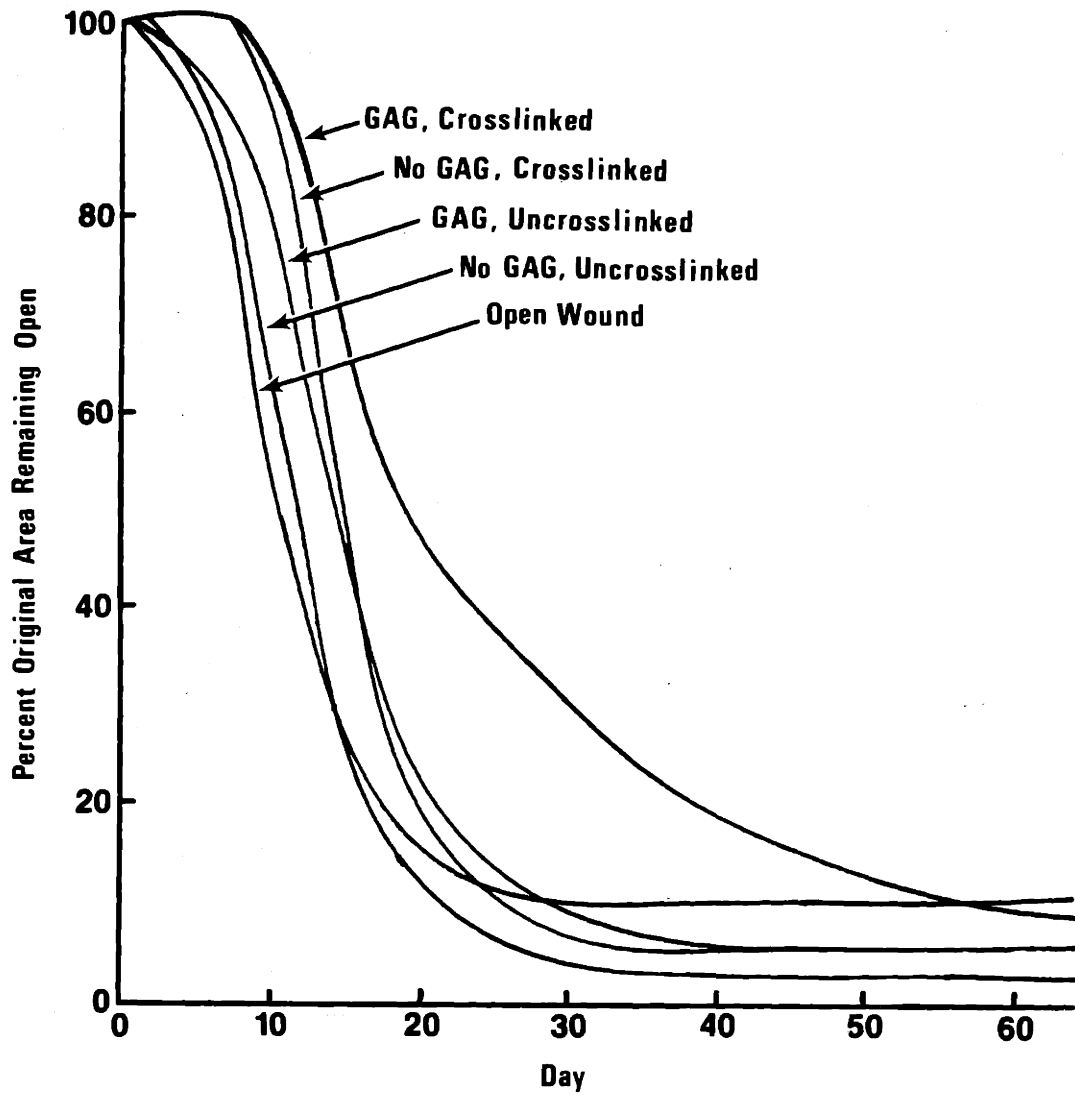


Figure 3-17: Composite Wound Contraction Curve

Table 3-XII: Linear Regression of Contraction Data

| Membrane | Slope (Wound area/day) | 50% Wound Closure | Correlation |
|-----------------------|---------------------------|----------------------|-------------|
| GAG, Crosslinked | -3.9 | 19 | -.99 |
| No GAG, Crosslinked | -5.6 | 16 | -1.0 |
| No GAG, Uncrosslinked | -5.9 | 12 | -.99 |

Chapter 4

Discussion

4.1 Effects of Glutaraldehyde Crosslinking and Chondroitin-6-Sulfate Upon the Mechanical Properties and In Vivo Response of an Artificial Skin

Prior to discussion of the *in vivo* response of the guinea pig model to the artificial membranes, the consistency of select material properties of the different membranes must be determined. The select variation of material properties by processing parameters allows the direct correlation of *in vitro* behavior to *in vivo* response.

The percent solids obtained for the GAG and No GAG slurries prior to freeze drying are comparable; the 0.51% solid content of the GAG slurry consistent with the 0.50% solid content cited in the standard protocol¹⁵. The 0.33% solid content of the No GAG slurry is explained both by the lack of glycosaminoglycan in the slurry and the removal of the high density collagen pellet due to contamination. No solid was found in the supernatant.

The helicity calculations for the collagen molecules found in the GAG and No GAG slurries prior to freeze drying indicate both have a high degree of helicity. The 95% helicity of the GAG slurry is greater than the 79% helicity of the No GAG slurry. This may be due to the influence of the glycosaminoglycan upon the infrared spectrum. The results indicate that both collagen slurries demonstrate a high helicity.

The length average banding values of 1.26 and .60 obtained for the pH 3 GAG and No GAG slurries respectively compare to the 1.00 value obtained by Sylvester²⁰ for a pH 3 GAG slurry. The presence of glycosaminoglycan in the slurry may increase the banding by maintaining some crystallization of the collagen through bonding of neighboring molecules.

Scanning electron photomicrographs revealed average porosities of 160 μm for both the GAG and No GAG membranes following freeze drying. The raised shelf temperature (-20°C) of the freeze drier during the freezing of the No GAG slurries allowed the viscous No GAG slurry to freeze slower. Pore formation is dependent upon the rate of nucleation of ice crystals and the rate of diffusion of water molecules. As increased viscosity reduces the diffusion of water molecules, nucleation was hindered. The increased shelf temperature permitted slower freezing, allowing additional time for water diffusion to the site of nucleation¹⁰.

The scanning electron photomicrographs demonstrated the presence of a channelling structure in the No GAG foams which was not found in the GAG foams. Again, the increased viscosity of the No GAG slurry may alter the freeze drying kinetics. The channelling was assumed not to significantly alter the contraction behavior of wounds treated with the No GAG foams as the porosity, upon which cellular infiltration is dependent, was consistent to that of the GAG foams.

The presence or absence of glycosaminoglycan in the collagen matrix crosslinked with .25% glutaraldehyde did not significantly alter the crosslink density. The 9,500 daltons between crosslinks found in the GAG, crosslinked membrane was within error of the 12,000 daltons found between crosslinks in the No GAG, crosslinked specimen. The values compare to the 8,000 dalton

value obtained by Chen¹⁰ for GAG, crosslinked membranes. Both sets of values fell in the normal range of 8,000 to 20,000 daltons for control Stage I material.

The deletion of the glutaraldehyde crosslinking of the No GAG membrane decreased the degree of crosslinking by increasing the molecular weight between crosslinks to 40,000 daltons. This value compared the the 39,000 dalton value obtained by Chen¹⁰ for GAG, uncrosslinked membranes. The results indicated the crosslink density of the material was independent of the glycosaminoglycan content at levels of 8% or less, but dependent upon the degree of glutaraldehyde crosslinking.

$1/\tau$ testing performed on the GAG, crosslinked and No GAG, crosslinked membranes by Wilson¹³ verified the finding by Huang¹² that the presence of glycosaminoglycan in the collagen matrix decreases the collagenase degradation rate. $1/\tau$ testing was not performed on the No GAG, uncrosslinked membrane. As Huang¹² also demonstrated a rapid increase in collagenase degradation with the decrease of crosslink density, the No GAG, uncrosslinked membrane will be assumed to exhibit an increased collagenase degradation rate comparable to that of the No GAG, crosslinked membrane.

The glycosaminoglycan content of the membranes was examined following wet processing and twenty four hour storage in 70% isopropanol. Both the No GAG, crosslinked and No GAG, uncrosslinked membranes indicated 0.35% glycosaminoglycan content. A value of 1% glycosaminoglycan content for a No GAG, collagen complex was obtained by Stasikelis²⁴. The value is attributed to background noise in the assay due to the presence of glycosaminoglycan in the native collagen prior to processing.

The GAG, crosslinked and No GAG, uncrosslinked membranes contained 2.67% and 3.01% glycosaminoglycan respectively. Elution of glycosaminoglycan occurred during wet processing, as the glycosaminoglycan content of specimen after dehydrothermal treatment prior to wet processing is approximately 8.0%. The consistent values indicated the crosslinking did not effect the retention of glycosaminoglycan by the membranes.

Both the elution of glycosaminoglycan during processing and the independence of glycosaminoglycan retention upon glutaraldehyde crosslinking countered the results obtained by Rubenstein^{25,26}. The results revealed the glycosaminoglycan retention of collagen-GAG membranes is strongly dependent upon the ionic nature of the elution solution. Deionized water was found to induce 100% retention of glycosaminoglycan in crosslinked collagen-GAG complexes while 19% retention was obtained with saline²⁶. Further, glutaraldehyde crosslinking was seen to increase glycosaminoglycan retention during elution in ionic solution²⁶. Examination of the wet processing stages did not reveal the usage of solutions with significant ionic strengths. The alcohol in the 70% isopropanol used for storage of the artificial skin after processing may induce the glycosaminoglycan elution due to chemical alteration of the collagen. Further work must be performed to further examine this result as no studies have yet been completed in this area.

The material testing demonstrated the properties of the GAG, crosslinked and No GAG, crosslinked membranes differed significantly only in *in vitro* collagenase degradation rate. The GAG, crosslinked and No GAG, uncrosslinked membranes varied in both crosslink density and *in vitro* collagenase degradation rate. The select variation of material property by processing variable allowed the correlation of processing variable to *in vitro*

behavior to *in vivo* response.

The deletion of glycosaminoglycan in the crosslinked membranes was seen to increase the rate of wound contraction by a factor of 1.4. Utilizing the linear regressions of the contraction curves seen in Table 4-I, the GAG, crosslinked membranes contracted at a rate of -3.9% wound area/day while the No GAG, crosslinked membranes underwent contraction at a rate of -5.6% wound area/day. The contraction rate of -3.9% wound area/day obtained for the GAG, crosslinked membranes compared well to the -3.7% wound area/day obtained by Chen¹⁰ for similar material.

Table 4-I: Contraction Data

| Membrane Type | Slope (Wound Area/Day) | 50% Wound Closure | Onset of Contraction |
|----------------------|---------------------------|----------------------|-------------------------|
| GAG,Crosslinked | -3.9 | 19 | 14 |
| No GAG,Crosslinked | -5.6 | 16 | 14 |
| GAG,Uncrosslinked | -5.3 | 16 | 5 |
| No GAG,Uncrosslinked | -5.9 | 12 | 5 |
| Open Wound | -7.2 | 11 | 5 |

As the onset of wound contraction for the two membranes was approximately Day 14, the shift in the rate of wound contraction was responsible for the three day delay in 50% wound closure demonstrated by the control GAG, crosslinked material. 50% wound closure seen on day 19 by the control material compared favorably to the day 20 result obtained by Chen¹⁰. The No GAG, crosslinked membrane may be undergoing degradation by the body more rapidly than the GAG, crosslinked membrane.

The histological findings mirrored the findings of the wound contraction data. An increased intact collagen matrix was seen for the GAG, crosslinked

membrane on days 21 and 28. Further, neodermal regeneration in the bottom of the GAG membrane was greater than the No GAG specimen. Epithelialization of the wound surface was consistent for the two materials.

The chemical mechanism behind the increased wound contraction of the No GAG, crosslinked membrane may be the collagenase degradation rate. *In vitro* testing demonstrated the dependence of collagenase degradation upon the glycosaminoglycan content of the collagen matrix.

Tissue collagenase is an enzyme produced by the body which specifically cleaves peptide bonds in the helical regions of collagen molecules. The cleavage allows the helix to uncoil; opening the collagen molecule for enzymatic attack and degradation²⁷.

The presence of glycosaminoglycan in the collagen matrix provides additional intermolecular bonding of the collagen helices due to electrostatic interaction with the collagen strands¹¹. As proposed by Chen¹⁰, the additional bonds in the collagen helix may reduce the degradation rate by two mechanisms. First, the presence of glycosaminoglycan bonds may hinder the migration of the tissue collagenases to the specific cleavage sites in the collagen helix. Secondly, the additional intermolecular bonds may further strengthen the helix while the peptide bonds are being cleaved by collagenase. This would prevent the helix from uncoiling as rapidly, reducing the rate of enzymatic attack and degradation²⁸.

The deletion of both glycosaminoglycan and glutaraldehyde crosslinking increased the contraction rate by a factor of 1.5. The No GAG, uncrosslinked membranes demonstrated a -5.9% wound area/day contraction rate. The value is greater than both the -5.3% wound area/day contraction rate obtained by

Chen¹⁰ for GAG, uncrosslinked membranes and the -5.6% wound area/day contraction rate of the No GAG, crosslinked membranes. The differences between the contraction rates of the membranes with one processing variation and the control sum to a greater value (3.7%) than both the difference between the No GAG, uncrosslinked membrane and the control (2.0%) and the difference between the open wound and the control (3.3%). Utilizing this result, the two processing variables appear not to be independently additive in delaying contraction.

The onset of wound contraction for the No GAG, uncrosslinked membranes occurred on Day 5; significantly earlier than the onset of contraction on day 14 demonstrated by the crosslinked membranes. Work by Chen¹⁰ with GAG, uncrosslinked membranes also indicated an early onset of wound contraction. Both the advance of the onset of wound contraction and the increased contraction rate caused the No GAG, uncrosslinked membranes to exhibit 50% wound closure on Day 12, seven days earlier than the control membranes. The seven day delay demonstrated by the No GAG, uncrosslinked membranes is consistent with the addition of the four day delay seen with GAG, uncrosslinked membranes¹⁰ and the three day delay seen with the No GAG, crosslinked membranes. As glycosaminoglycan content plays a role in contraction kinetics after day 14, glutaraldehyde crosslinking appears to be instrumental in affecting both early and late wound contraction.

The histological sections of the No GAG, crosslinked membranes revealed increased degradation of the collagen matrix compared to the crosslinked membranes. Little collagen regeneration was seen in the base of the matrix. Epithelialization was complete by day 14. By day 28, the upper portion of the collagen matrix was compressed together by the surrounding tissue; the

matrix forming a trapezoid in the woundbed. The compression of the matrix may be due to extreme degradation of the collagen support.

Treatment with glutaraldehyde has been demonstrated to induce crosslink bridges between the lysine residues of neighboring collagen α -strands²⁰. The crosslinking of the collagen helices may reduce the collagenase degradation rate of the collagen membrane by increasing the intermolecular bonding between the collagen strands in the individual helices. The glutaraldehyde bridges would both partially obstruct the collagenase cleavage sites and maintain the structure of the helix during cleavage of the peptide bonds.

By processing a Stage I artificial skin without glutaraldehyde crosslinking and glycosaminoglycan, the collagen matrix is liable to faster degradation due to reduction of intermolecular bonding in the collagen helix. The No GAG, uncrosslinked membranes exhibited wound contraction behavior approximating open wound contraction. However, the approximation was not complete. Other material properties of the artificial skin such as siliconization may be the final variables affecting the overall shift in wound contraction.

The correlation of *in vitro* behavior to *in vivo* response by select variation of processing variables partially allowed the mechanism of wound contraction regulation to be elucidated. Glutaraldehyde crosslinking and glycosaminoglycan content were seen to significantly delay the onset of contraction and reduce the contraction rate in an *in vivo* guinea pig model. Collagenase degradation, the material property affected by both glutaraldehyde crosslinking and glycosaminoglycan content, underlies the regulatory mechanism of wound contraction. The studies have demonstrated the factors which influence the collagenase degradation rate of the Stage I artificial skin will offer the greatest promise in the ultimate mechanical regulation of wound contraction.

Chapter 5

Conclusions

1.

The grafting of full thickness wounds on guinea pigs with crosslinked membranes varying only in glycosaminoglycan content revealed an increase in the rate of wound contraction due to the lack of glycosaminoglycan in the collagen matrix. As both the onset of wound contraction and the rate of epithelialization were consistent for the two types of membranes, the three day increase in 50% wound closure induced by the crosslinked membranes without glycosaminoglycan compared to the crosslinked membranes with glycosaminoglycan may be attributed to increased wound contraction rate affected by the lack of glycosaminoglycan.

2.

Uncrosslinked membranes which contained no glycosaminoglycan demonstrated an increased contraction rate compared to both crosslinked membranes with glycosaminoglycan and crosslinked membranes without glycosaminoglycan. The rate of epithelialization was comparable between the three types of membranes. The onset of wound contraction was seen to occur nine days earlier when the full thickness wounds were grafted with uncrosslinked membranes containing no glycosaminoglycan compared to results obtained with either type of crosslinked membrane. The seven day increase in 50% wound closure demonstrated by the uncrosslinked membranes containing no glycosaminoglycan compared to the crosslinked membranes containing

glycosaminoglycan may be attributed to the affects of the lack of glutaraldehyde crosslinking and glycosaminoglycan content upon both the increased rate of contraction and the earlier onset of wound contraction.

3.

The porosity of a collagen matrix can be controlled by regulation of the shelf freezing temperature during freezing. A higher freezing temperature induced slower freezing, allowing more time for nucleation of water crystals in the slurry. Upon freeze drying, the resultant pore size was larger than the pore structures seen at lower freezing temperatures.

References

1. Montgomery, B.J., "Consensus for the Treatment of the Sickest Patients You'll Ever See," *J. Am. Med. Assoc.*, 241:345 (1979)
2. Rudouski, W., *Burn Therapy and Research*, Baltimore, Johns Hopkins, 1976
3. Burke, J.F., Yannas, I.V., Quinby, W.C., Bondoc, C.C., and Jung, W.K., "Successful Use of a Physiologically Acceptable Artificial Skin in the Treatment of Extensive Burn Injury," *Ann. of Surg.*, 194:413 (1981)
4. Collins, J., Peacock, E., and Chvapil, M., "A New Collagen Sponge to Dress Open Wounds," *Surg. Forum*, 27:551 (1976)
5. Chvapil, M., Holusa, R., Kliment, K., and Stoll, M., "Some Chemical and Biological Characteristics of a New Collagen-Polymer Compound Material," *J. Biomed. Mater. Res.*, 3:315 (1969)
6. Spira, M., Fissette, J., Hall, W., Hardy, S.B., and Gerow, F.J., "Evaluation of Synthetic Fabrics as Artificial Skin Grafts to Experimental Burn Wounds," *J. Biomed. Mater. Res.*, 3:213 (1969)
7. Yannas, I.V., "Prompt, Long Term Functional Replacement of Skin," *Trans. A.S.A.I.O.*, 27:19 (1981)
8. Grillo, H.C., Watts, G.T., and Gross, J., "Studies in Wound Healing: I. Contraction and the Wound Content," 148:145 (1958)
9. Yannas, I.V., "Use of Artificial Skin in Wound Management," in *THE SURGICAL WOUND*, Peter Dineern, ed., Philadelphia: Lea & Febiger, 191, pg. 184
10. Chen, E., "The Effects of Porosity and Crosslinking of a Collagen Based Artificial Skin on Wound Healing," S.M. Thesis, Mechanical Engineering, MIT (1982)

11. Lindahl, U., Hook, M., "Glycosaminoglycans and their Binding to Biological Macromolecules," *Ann. Rev. Biochem.*, 47:385 (1978)
12. Huang, C., "Physiological Studies of Collagen and Collagen-Mucopolysacchride Composite Materials," Sc.D. Thesis, Mechanical Engineering, MIT (1975)
13. Wilson, R., "Effect of Strain and Glycosaminoglycan Content on the Degradation Rate of Collagen-based Membranes by Bacterial Collagenase," S.B. Thesis, Department of Mechanical Engineering, MIT (1983)
14. Komanowshy, M., et al, "Production of Comminuted Collagen for Novel Applications," *J. Am. Leather Chem.*, 69:410 (1974)
15. Skrabut, E., "Protocol for Collagen/GAG Foam," unpublished paper (1980)
16. Sung, N.-H., "Structure and Properties of Collagen and Gelatin in the Hydrated and Anhydrous Solid State," Ph.D. Thesis, Mechanical Engineering, MIT (1972)
17. Rubenstein, R., "Standardization of Collagen-Mucopolysacchride Composite Materials," M.S. Thesis, Mechanical Engineering, MIT (1977)
18. Elson, L.A., Morgan, W.T.J., "A Colorimetric Method for the Determination of Glucosamine and Chondrosamine," *Biochem.J.*, 27:1824 (1933)
19. Swann, D.A., Balazs, E.Z., "Determination of the Hexosamine Content of Macromolecules with Manual and Automated Techniques using the p-Dimethylaminobenzaldehyde Reaction," *Biochim. Biophys. Acta.*, 130:112 (1966)
20. Sylvester, M., "Thrombogenicity of Collagen," M.S. Thesis, Mechanical Engineering, MIT (1982)
21. Forbes, M., "Cross-Flow Filtration, Transmission Electron Micrographic Analysis and Blood Compatibility Testing of Collagen Composite Materials for Use as Vascular Protheses," M.S. Thesis, Mechanical Engineering, MIT (1980)

22. Yannas, I.V., Stasikelis, P., "Determination of Crosslink Density of Blood Vessel Protheses," unpublished paper, (1981)
23. Orgill, D., "The Effects of an Artificial Skin on Scarring and Contraction in Open Wounds," Ph.D. Thesis, Mechanical Engineering, MIT (1983)
24. Stasikelis, P.J., "Burn Dressings Based on Collagen: Structural Parameters Affecting Performance," S.M. Thesis, Mechanical Engineering, MIT (1979)
25. Rubenstein, R.H., "Standardization of Collagen Mucopolysaccharide Composite Materials," S.M. Thesis, Mechanical Engineering, MIT (1977)
26. Yannas, I.V., Burke, J.F., Gordon, P.L., Huang, C., Rubenstein, R.H., "Design of an Artificial Skin. II. Control of Chemical Composition," J. Biomed. Res., 14:107 (1980)
27. Stryer, L., BIOCHEMISTRY, W.H. Freeman and Company, San Fransisco, CA (1981)
28. Peacock, E.E., "Collagenolysis: The Other Side of the Equation," World J. Surg., 4:297 (1980)